Mass flow in hyphae of the oomycete *Achlya bisexualis*

A thesis submitted in partial fulfilment of the requirements for the Degree
of Master of Science in Cellular and Molecular Biology
in the University of Canterbury
by Mona Bidanjiri
University of Canterbury
2018

Abstract

Oomycetes and fungi grow in a polarized manner through the process of tip growth. This is a complex process, involving extension at the apex of the cell and the movement of the cytoplasm forward, as the tip extends. The mechanisms that underlie this growth are not clearly understood, but it is thought that the process is driven by the tip yielding to turgor pressure. Mass flow, the process where bulk flow of material occurs down a pressure gradient, may play a role in tip growth moving the cytoplasm forward. This has previously been demonstrated in mycelia of the oomycete *Achlya bisexualis* and in single hypha of the fungus *Neurospora crassa.* Microinjected silicone oil droplets were observed to move in the predicted direction after the establishment of an imposed pressure gradient. In order to test for mass flow in a single hypha of *A. bisexualis* the work in this thesis describes the microinjection of silicone oil droplets into hyphae. Pressure gradients were imposed by the addition of hyperosmotic and hypoosmotic solutions to the hyphae. In majority of experiments, after both hypo- and hyperosmotic treatments, the oil droplets moved down the imposed gradient in the predicted direction. This supports the existence of mass flow in single hypha of *A. bisexualis*. The Hagen-Poiseuille equation was used to calculate the theoretical rate of mass flow occurring within the hypha and this was compared to observed rates. To create a more streamlined system for future study, this thesis also describes Lab-on-a-Chip technology and the design of chips, which isolate single hyphae from the rest of the mycelium. While microinjection of oil was unsuccessful on these chips in the present study, with modification in the future this new system may produce a more controlled environment for the study of mass flow.

Table of Contents

List of figures

List of Tables

Abbreviations and definitions

F – actin	Filamentous actin
PYG	Peptone, yeast and glucose media
PM	Plasma membrane
ER	Endoplasmic reticulum
EE	Early Endosomes
ATP	Adenosine triphosphate
TeaR	Hyphal tip marker in *Aspergillus nidulans*
mod5	Hyphal tip marker in *Schizosacchromyces pombe*
mRNAs	Messenger RNA
SPK	Spitzenkörper
VSC	Vesicle supply center
nm	Nanometer
Arp 2/3	Actin-Related protein 2 and Actin-Related protein 3 complex
Formins	Group of proteins involved in polymerization of actin
Profilin	Actin binding protein
Cofilin	Actin binding protein
XMAP	Xenopus microtubule-associated protein
TIP proteins	Microtubule plus-end tracking proteins
γ – tubulin ring complex	Protein complex the nucleates microtubules at the centrosome
MTs	Microtubules
Bars	Metric unit of pressure
MPa	Mega Pascal
$PV = nRT$	Ideal gas equation
Ca^{2+}	Calcium ions
PEG	Polyethylene glycol
µm	Micrometer
min	Minute

K^+	Potassium ions
atmospheres	Unit of pressure
mps1 and pmk 1	Mitogen activated protein kinase genes
MAPK pathway	Mitogen activated protein kinase pathway
NMR	Nuclear magnetic resonance imaging
kPa	Kilopascal
^{14}C	Carbon 14 or radiocarbon
M	Molar (moles per liter)
±	Standard deviation
s^{-1}	Per second
Re	Reynold's number
MEMS	Microelectromechanical systems
PDMS	Polydimethylsiloxane
LOC device	Lab-on-a-chip device
µN	Micronewton
in vivo	Within the living
in vitro	Outside the living organism
mm	milli-meter
gL^{-1}	Grams per liter
%	Percent
^0C	Degrees Celsius
LAF	Laminar air flow
mL	milli-Liters
Hrs	Hours
I.D.	Inner diameter
O.D.	Outer diameter
ETFE	Ethylene-tetrafluroethylene
VU	Voltage units
cm	Centimeter
µL	Microliter
mmol/Kg	Millimole per kilogram

mOsml/Kg	Milliosmol per kilogram
"	Inches
w/w	weight per weight
IPA	Isopropyl alcohol
ROI	Region of Interest
SEM	Standard error mean
n	Number
pH	Potential of hydrogen
H^+	Protons
BS	Basal salt
Gd^{3+}	Gadolinium
TEA	Tetraethylammonium
pA	Amplitude
mM	Millimoles
NaCN	Sodium cyanide
Pa	Pascals
W	Watts

Chapter 1. Introduction

1.1 Filamentous eukaryotic microorganisms: Fungi and Oomycetes

Most ecological niches are occupied by microorganisms, including filamentous microbes like fungi and oomycetes (Stajich et al., 2009). They both possess a dominant vegetative structure, the hypha, which is cylindrical in shape and slightly tapered towards the apex (Money, 2011). This similarity and the fact that they both display absorptive nutrition has prompted their general taxonomic grouping and use in comparative studies but in fact evidence obtained from phylogenetic studies suggest that they belong to different eukaryotic kingdoms (Lévesque, 2011). Due to their saprotrophic nature they play key roles in most ecosystems acting as decomposers and recyclers of organic material (Evans & Hedger, 2001). Although fungi and oomycetes are placed in two distant branches of the eukaryotic phylogenetic tree their hyphal mode of growth, mode of nutrition and associated infection structures such as haustoria and appressoria are thought to have arisen through convergent evolution. Also, the cell wall degrading enzymes in both species are similar in sequence and action (Latijnhouwers, de Wit, & Govers, 2003).

1.2 Fungi vs Oomycetes

As mentioned above, even though oomycetes share several morphological and nutritional characteristics with the fungi, they belong to a different eukaryotic kingdom. Phylogenetic studies of these two organisms place the oomycetes amongst the Stramenopiles (heteroknot) in the kingdom *Chromista* and their closest relatives include the diatoms, golden-brown algae and brown algae. In contrast members of the kingdom Fungi (uniknots) are more closely related to animals and choanoflagellates. Despite their morphological similarity, oomycetes and fungi differ in several characteristics including their mode of development, cellular features and biochemistry (Beakes, Glockling, & Sekimoto, 2012; Latijnhouwers et al., 2003). The absence of ergosterol in the cytoplasmic membrane of oomycetes is one such difference, rendering them resistant to most fungicides. Other differences include the composition of cell wall where oomycetes primarily contain cellulose rather than chitin, which is abundant in the fungal cell wall. This renders oomycetes resistant to most chitin inhibitors (Bartnicki-Garcia, 1968; Latijnhouwers et al., 2003). Oomycetes are coenocytic, unlike fungi which possess septa, cross walls with pores which help in separating cells within the hypha. The coenocytic nature of

oomycetes may be behind the evolution of a wound response, which involves the formation of callose plugs. These plugs enable the maintenance of cell integrity and internal pressure in instances of cell wall damage. It also stops the leakage of internal cellular contents out of the hyphae. The main factors thought to be involved in wound response are F-actin and Ca^{2+} levels. Both these components have been associated with septa formation in fungi (Levina, Heath, & Lew, 2000).

Hyphal structure

Hyphae are cylindrical structures with either a hemi-ellipsoidal or hemispherical apex. They are thought to undergo orthogonal expansion, enabling both fungi and oomycete to absorb maximum nutrients from the surrounding milieu. These structures have a high surface area to volume ratio that ensures efficient nutrient uptake. Their shape (essentially like drill bits) also enables them to penetrate a wide variety of substrata, which may include both plant and animal forms (Riquelme, 2013; Steinberg et. al, 2017). These filaments in turn form large networks or mats termed mycelium, which are made up of repeatedly branching hyphae and, depending on the species, these mycelia can extend for several kilometres. (Arkowitz & Bassilana, 2011; Lévesque, 2011; Money, 2008). Though hyphal growth is usually linear, external factors such as nutrient availability, the change in substrate topography or magnetic fields could affect the directionality of this mode of growth (Arkowitz & Bassilana, 2011; Goriely & Tabor, 2008).

1.3 Oomycetes

The formal name of these organisms, oomycota, is descriptive of their resemblance to eggs. While oomycetes are commonly known as water molds they are found in both aquatic and terrestrial habitats (Beakes et al., 2012; Lévesque, 2011). Currently, it is accepted that they originated as obligate sea parasites, which eventually evolved into saprotrophic land forms (Lévesque, 2011). They can reproduce either sexually, asexually or in both ways. In most cases of asexual reproduction there is production of biflagellate zoospores, while sexual reproduction is dependent on the formation of oospores, which survive extreme weather conditions (Latijnhouwers et al., 2003).

Beneficial effects of oomycetes

Oomycetes and fungi are key components of most ecosystems on the planet, degrading dead and decaying organic matter to recycle useful components such as carbon, nitrogen and phosphorus. This is essential for nutrient recycling (Riquelme, 2013). Two aquatic examples of this are *Halophytophthora*, which grows and reproduces in brackish water of mangroves and is a fundamental decomposer of leaf waste (Nakagiri, 2000) and members of the *Saprolegniales*, which inhabit freshwater habitats acting as decomposers for aquatic debris including waterlogged twigs and leaves, insect cast offs and decomposing aquatic organisms (Dick, 1969).

The pathogenic capacity of some oomycetes can also be used to our advantage. *Pythium oligandrum* has been used as a biocontrol, helping fight infections within plants by colonizing root cells. They are known to provide protection either directly or indirectly to the host plant against a large range of pathogens, and are especially important as they do not harm the valuable microflora present in the root system (Gerbore et al., 2014). The facultative parasite *Lagnidium giganteum* can infect and kill mosquitoes and hence their larvae are frequently introduced as biocontrol agents (Kamoun, 2003). Oomycetes, like fungi infect their hosts by attaching themselves to external surface of the cells using a glue-like substance. These are synthesized in aqueous environments and offers them adherence to the host. The entire composition of this glue is not known but due to their strength, biocompatibility and ability to adhere in aqueous environments, they could have industrial applications acting as templates to produce commercial models, which could be used in medicine as natural sealants (A. M. Smith & Callow, 2006).

Oomycetes as parasites and pathogens

While these microbes are key components of ecosystems owing to their saprotrophic nature, some species of oomycetes are parasitic and have the potential to become pathogenic. These can cause devastation by infecting different host organisms, including insects, plants, fishes and mammals (Latijnhouwers et al., 2003). The rampant spread of these diseases is influenced by factors such as importation of cultivars from other countries, climate change and the change in habitat. Some of the well-known oomycete diseases include blight in plants, saprolegniasis in fish and pythosis and lagenidosis in mammals (Bebber & Gurr, 2015; Lévesque, 2011;

Li et al., 2010; Mendoza & Vilela, 2013). The Irish potato blight is perhaps the most well-known case of the impact of oomycetes on human affairs in plants, in which *Phytophthora infestans* had devastating effects on the potato crop and caused the mass migration of a high proportion of the population of Ireland in the 1800s (Yoshida et al., 2013). The indigenous Māori of New Zealand, who implemented horticulture at the time also incurred major losses due to damage of crops caused by this disease (G. F. Harris, 2006). Another oomycete *Phytium insidiosum,* which has been identified as the causative agent of mycosis, has had dramatic effects infecting horses and cattle. They infect their hosts by formation of zoospores in aquatic habitats, but could also inhabit swampy land where agriculture is practiced in countries such as Thailand, causing disease in livestock and agricultural plants. Unfortunately, huge losses have been incurred due to this infection. Their other hosts include human beings who develop the disease of pythosis (Lévesque, 2011).

Structures of infection

Infective oomycetes, like the fungi, can produce specialized infection structures such as appressoria, which can form from a cell divided by a false septum. In addition, some biotrophic oomycetes produce haustoria, which are collar-like structures around the hypha filled with electron dense material, which help in the absorption of nutrients from the host organism (Bebber & Gurr, 2015; Latijnhouwers et al., 2003; Mendoza & Vilela, 2013; Thines & Kamoun, 2010). One of the more unique forms of infection in oomycetes occurs in the genus *Haptoglossa,* in which the parasitic lifestyle is achieved by them injecting themselves into their host animals using specialized cells called ‘gun’ cells (Hakariya, Masuyama, & Saikawa, 2002).

The *Hyaloperonospora Arabidopsis,* which infects the plant *Arabidopsis thaliana* infect the roots of this plant via oospores present in the soil. They also produce sporangiophores, which are dispersed aerially and could land on leaf surfaces. These spores then produce germ tubes, which eventually form hyphae with the appressoria and invade host tissue. After invading the epidermis layer, they produce specialized structures called haustoria. This structure absorbs nutrients from host tissue. Effectors are secreted by these structures, which reduce host defenses (Kamoun et al., 2015).

The *Achlya* genus

Members of the oomycete genus *Achlya* belong to the order *Saproleginales*, which as described above are a group of pathogens that can infect fishes and their eggs causing huge economic loses to the aquaculture industry. Some pathogens in this genus such as *Achlya conspicua* and *Achlya klebsiana* also infect terrestrial and aquatic plants (Srivastava, 1967). *Achlya bisexualis*, which forms the basis of this research, can cause ulcerative mycosis in fish (Fugelstad, 2008).

Unlike the fungi where several species have been used as model organisms, for example, *Saccharomyces cerevisiae*, *Schizosaccharomyces pombe*, *Neurospora crassa* and *Aspergillus nidulans*, there are no model species for oomycetes. Several key studies have investigated tip growth and turgor regulation in the oomycetes using *A. bisexualis* (Money & Harold, 1993; Randall et al., 2005; Walker et al., 2006; Yu, Jackson, & Garrill, 2004). Most importantly this species has been used to investigate mass flow in its mycelia (Muralidhar et al., 2016), hence it is the species that has been used in the experiments described in this thesis. *A. bisexualis* grown in PYG media on a petri-dish is represented in Figure 1.1.

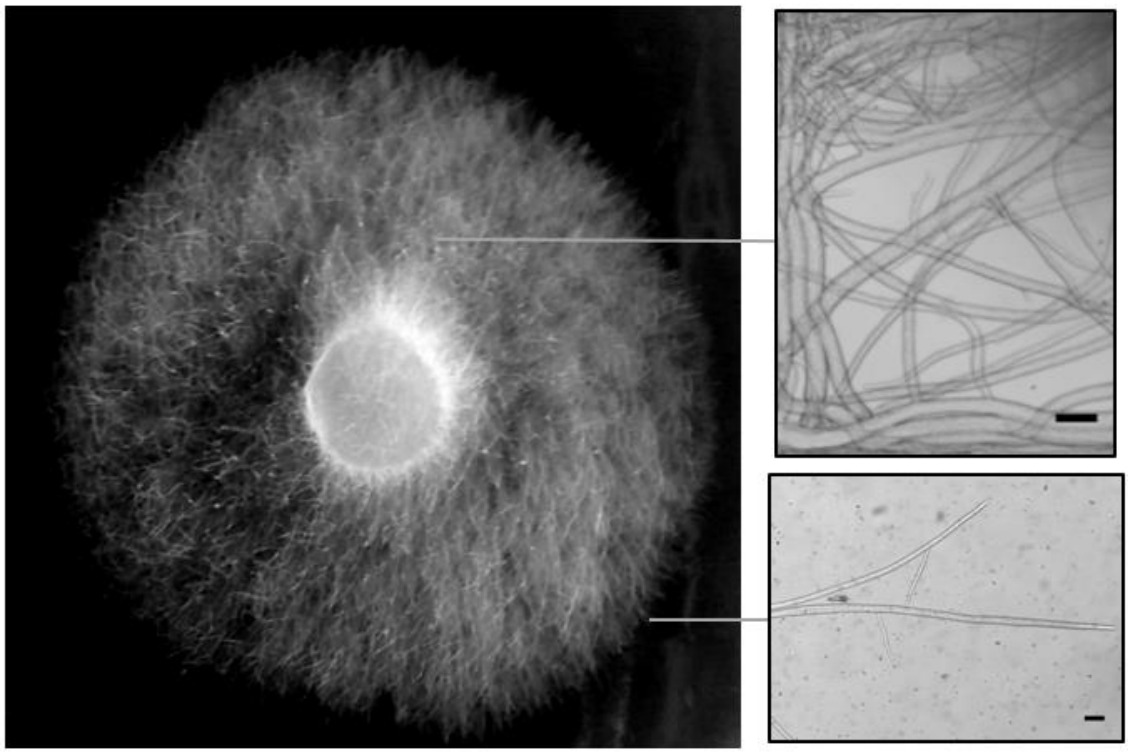

Figure 1.1: *Achlya bisexualis* grown on PYG media. The growth occurs from an inoculation plug placed at the center of an agar plate. The upper inset is of a mass of hyphae that make up the mycelium observed through a 4 X objective lens. The lower inset image is of hyphae at the edge of the mycelium again observed through a 4 X objective lens. Scale bar 50 μm.

1.4 Tip growth - Overview

As mentioned previously, the main commonality shared by fungi and oomycetes is that their main vegetative structure is the hypha and that these extend via the process of tip growth. Tip growth was first proposed as an orthogonal growth pattern by Reinhardt in 1892 (Riquelme, 2013). Subsequent studies conducted on *Mucor rouxii* supported the ideas of Reinhardt, with experimental evidence suggesting maximal growth occurred at a distance of approximately 1 µm from the apical tip (Bartnicki-Garcia & Lippman, 1969).

Tip growth, which is a form of polarized growth, is not limited to hyphal cells alone as it also occurs in root hairs and pollen tubes of plants, algal rhizoids and moss protonemata. In each case, tip growth serves the purpose of elongation and penetration, for example delivering pollen to the ovule via the pollen tube or penetration of soil by roots for absorption of nutrients. Amongst these, hyphal filamentous growth is thought to be the only case where growth effectively occurs indefinitely when presented with appropriate conditions (Arkowitz & Bassilana, 2011; Lew, 2011; Riquelme, 2013). Since substantial amounts of, and evenly distributed nutrients are provided under laboratory conditions for the growth of these organisms, in the environment nutrient distribution is likely to be more heterogenous and the elongation of hyphae is required to procure nutrition (Steinberg et al., 2017).

1.5 Polarity establishment and maintenance

Polarized growth is thought to be a function of two fundamental processes namely polarity establishment (i.e. cellular symmetry) and its maintenance (S. D. Harris, 2011; Riquelme, 2013). Even though spores and hyphal branches present apolar growth, this could be switched to a polarized form once growth axis stabilization is achieved. Evidence suggests that there might be internal mechanisms for localized cell surface expansion and cell wall deposition. This could include the recruitment of morphogenetic machinery at the site of growth axis establishment. Although, certain external cues, such as the release of pheromones might abrogate this mechanism, as was observed in *Saccharomyces cerevisiae* and *Saccharomyces pombe* (Chang & Peter, 2003). While signaling pathways might contribute in such processes, evidence is lacking. Multiple growth axes could be established simultaneously within a hypha, leading to lateral branching and then formation of the mycelial structure (S. D. Harris, 2008). The process

of translocation of components involved in tip growth (membranes and proteins) to the hyphal apex takes place after the establishment of a growth site and growth axis, which takes place by using the cytoskeletal network. Hence the formation of this axis is considered to be the basis of hyphal growth (Steinberg et al., 2017).

While several morphogenes have been identified and these may provide the information required for molecular building blocks of a hyphal structure, their identification has failed to explain the assembly and functionality, which leads to formation of a complex hyphal structure (Riquelme, 2013; Steinberg et al., 2017). This aspect of tip growth has relied instead on studies where the coordinated action of multiple enzymes, cytoskeletal elements and potential markers have been investigated. For example; septins, which are components of the cytoskeletal machinery are suggested to be critical in lateral branching by enabling specification and/or stabilization of new polarity axes. Hyphal tip markers such as TeaR in *A. nidulans* and mod 5 cells in *S. pombe* have been identified in regulation of cytoskeletal machinery (Takeshita et al., 2008). Evidence in *Aspergillus* species suggests that nuclear division and polarity establishment occur simultaneously (Fiddy & Trinci, 1976; Steinberg et al., 2017).

1.6 Exocytosis during tip growth

Fungal tip growth studies suggest that the components involved in the construction of the cell wall such as cell wall synthases, their substrates and the membranes required for the process of expansion are synthesized within the cell and then transported to the plasma membrane (PM) (Bartnicki-Garcia & Lippman, 1972). Their export is thought to be primarily driven by the movement of vesicles, which undergo exocytosis at the apex and upon fusing with the PM, the synthases become activated as they are integrated within it. The process of exocytosis at the apex, was suggested after observations were made in fungi which failed to establish polarity when they possessed mutations in regulators of exocytosis (S. D. Harris et al., 1999; Peñalva et al., 2012).

Golgi apparatus and its regulation

The Golgi within these organisms resemble the cisternae of eukaryotic Golgi apparatus (Wooding & Pelham, 1998). These organelles are considered critical in conventional secretory pathway of proteins, although, the entire mechanism of protein transport from their sites of production on the endoplasmic reticulum (ER) to their destination on the PM is not clearly understood. However, a model is proposed to explain the regulation of such transport called 'cisternal maturation' model (Losev et al., 2006). It suggests that the cargo of proteins from the ER exit, and are then loaded onto the Golgi till the lipid and protein content is converted. Eventually, this leads to them being compositionally competent to split into carrier vesicles headed for the endosomes and PM. However, this model fails to account for the microtubular connections known to be associated with such transport and the budding of carriers at different stages due to rapid separation possibly triggered by domains of variable lipid content (Steinberg et al., 2017).

1.7 Endocytosis and tip growth

As mentioned above, exocytosis is involved in tip growth by transporting a combination of cell wall synthesizing and degrading factors to the apical tip. About two decades ago the process of endocytosis was described in fungi for the first time (Riquelme et al., 2007; Vida & Emr, 1995). In experiments carried out with the lipophilic marker dye FM4-64 in a few species of fungi, the dye was taken up and transported to fungal vacuoles. Observations suggest this was due to the formation of endocytic transport vesicles termed early endosomes i.e. EE, which eventually underwent maturation forming late endosomes. The degradation of these endosomes takes place in fungal vacuoles (Steinberg, 2014). The initial sorting of material, which is to be recycled and sent back to the PM takes place within the EE. Filamentous species are characterized by the presence of a motile EE, which is considered to be due to the hydrolysis of ATP (Read & Kalkman, 2003; Steinberg et al., 2017; Vida & Emr, 1995). The motility of EE is achieved by movement of the motor proteins, kinesin and dynein moving along microtubules (Steinberg et al., 2017).

Growing evidence suggests that there might be additional roles of EE's. Various organelles and cellular components such as mRNAs, polysomes, peroxisomes, lipid droplets and the ER are suggested to hitchhike upon the EE. These organelles are transported to different parts of the cell on the EE (Salogiannis & Reck-Peterson, 2017; Steinberg, 2014). This theory is reinforced from findings obtained in mutant EE studies where cellular components were concentrated at the hyphal tip. Other roles might include the biosynthesis of melanin and aggregation of heat shock proteins (Lemmon, 2003; Steinberg et al., 2017).

1.8 Models of tip growth

Three primary models have been proposed to explain the process of tip growth, which include the vesicle supply center model, the steady state model and the role of cytoskeleton in tip growth. The vesicle supply center model proposed by Bartnicki-Garcia suggests that the Spitzenkörper plays a central role in transport of vesicles from the Golgi to PM (Riquelme, 2013).

The Spitzenkörper

Early observation on several fungi using phase contrast microscopy studies identified apical bodies and apical vesicle crescents (Hoch & Staples, 1983; Lehmler et al., 1997; Löpez-Franco & Bracker, 1996). Dense vesicular structures, which were first observed in *Coprinus sp*, were later termed the Spitzenkörper (SPK) and nine different SPK patterns have been observed in various fungi. Analysis of the components of the SPK reveal vesicles, ribosomes, actin microfilaments and an unidentified amorphous substance. It has been suggested that the SPK acts as a vesicle centre for transport of cell wall biosynthesizing enzymes like chitin and glucan synthases (Riquelme et al., 2007; Verdín, Bartnicki-Garcia, & Riquelme, 2009). The SPK is also suggested to act as a station for the transfer of cytoplasmic microtubules, which are considered essential for hyphal morphogenesis, SPK stability and the long-distance transport of vesicles onto actin microfilaments, which are further proposed to connect at the hyphal tip by cell end markers (Löpez-Franco & Bracker, 1996; Riquelme, 2013). In some fungi and in the oomycetes there is no distinct SPK although these do have an amassing of vesicles at the hyphal tips. Findings suggest that these vesicles are needed for morphogenesis, development, pathogenicity and the transfer of chitin synthases to the apical tip (Riquelme, 2013; Steinberg et al., 2017).

Vesicle supply center

The mechanism for tip growth involves manufacture and transfer of cell wall material within vesicles through exocytosis and endocytosis, but their transport from the Golgi to PM is not clearly understood. The discovery of the SPK in *N. crassa* and identification of cell wall production enzymes within its core, strengthened the theory that the SPK might perform the function of a vesicle supply centre (Riquelme et al., 2007; Verdín et al., 2009). This centre transfers cell wall degrading and synthesizing enzymes transported within vesicles, which move to the apex by the process of exocytosis. While germ tubes of *N. crassa* and some fungi and oomycetes do not have a defined SPK, it may be that these have a lower requirement for vesicular exocytosis at the tips. However, this is debatable since the SPK in *N. crassa* is thought to be most robust while their germ tubes lack a SPK, and that many oomycetes grow at similar rates and thus have a requirement for exocytosis to many fungi (Riquelme, 2013).

Currently, the more complex three-dimensional model of VSC is accepted according to which the SPK is held in place or displaced from its position due to the role of cytoskeleton while turgor will allow cell expansion at the surface. A hyphoid equation

$y = x \cot (x\ V/N)$ [N – vesicles involved in cell building per unit of time, V – rate of movement of VSC],

has been derived using computer simulations of fungal morphogenesis and suggests that due to the SPK a hypha can be produced by the movement of the VSC in a linear fashion while vesicles exocytose. This is a question other models have failed to answer (Bartnicki-Garcia & Gierz, 1993; Reynaga-Peña, Gierz, & Bartnicki-Garcia, 1997). By altering values in the equation, different cell shapes of hypha can be generated including branching and spore formation. However, as with most biological models it makes several assumptions. The absence of the SPK in other tip growing organisms has questioned the universality of the model, though evidence might suggest that some of them might possess unspecialized vesicular masses (Riquelme, 2013; Steinberg et al., 2017).

Vesicles

Two types of vesicles are involved in transport of cellular components, micro-vesicles, which are ~ 40 to 50 nm in diameter and macro-vesicles with ~ 100 nm diameters. While biochemical evidence proposes that some micro-vesicles carry enzymes such as chitinases to the PM, the components of macro-vesicles is not known. However, early evidence suggests that they might transport glucanases or other cell wall building enzymes (Riquelme, 2013). The system for transport of these vesicles from their site of synthesis to the SPK is thought to be dependent on microtubules (MT) and over shorter distances actin microfilaments (Riquelme, 2013; Steinberg et al., 2017).

Steady state model

Another model that attempts to explain some of the processes in tip growth is the steady state model, which describes the plasticity of the wall where growth occurs. According to the steady state model proposed by Wessels, the extension of a cell occurs because of the plastic wall of the hyphal tip and the plasticity occurs due to the addition of cell wall building material by the process of exocytosis at the apex, which eventually become cross-linked in the sub-apical region. Thus, in the sub-apical regions the wall is elastic rather than plastic and does not yield to turgor pressure. The steady-state model does not support the idea of cell-lytic enzymes being involved during the process of tip growth (Wessels, 1988).

The cytoskeleton and tip growth

Actin and myosin along with associated proteins such as Arp 2/3 complex, formins, profilin and cofilin, microtubules and associated motor proteins such as the gamma tubulin ring complex, XMAP, TIP proteins together constitute the cytoskeletal network. Working together the entire apparatus coordinates the maintenance of cytoplasmic organization, controls organelle positioning and movement while also playing an important role in tip growth and morphogenesis (Steinberg et al., 2017).

Evidence has shown that actin microfilaments are present at the tips of fungi and oomycetes suggesting they might have a role in tip growth (Bartnicki-García, 2002). They have been associated in maintaining polarity, the movement of organelles and other cellular components within the hyphal cell. In association with actin, myosin is suggested to participate in transport of

vesicles leaving the site of Golgi (Howard, 1981). It has also been suggested to play a role in the control of tip yielding during invasive hyphal growth (Suei & Garrill, 2008).

Microtubules are essential for the process of exocytosis and endocytosis within the hyphal cell. They are made up of proteins heterodimers (tubulin heterodimers). These associate from end to end and have an inherent polarity. Thus, the MTs have a plus and minus end. The motor proteins move with defined directionality along the MTs (kinesin predominantly to the plus end, dynein predominantly to the minus end). The motor proteins bind allowing for the movement of vesicles, organelles and other cellular components. The process of translation of some mRNAs is thought to occur while moving on these MTs, for example the mRNA encoding septins can undergo translation during movement on MTs. Septins play a role in maintenance of cell shape and the process of exocytosis (Steinberg et al., 2017).

1.9 Turgor

In addition to the molecular and cellular processes, described above, another important player in tip growth is turgor pressure, which is thought to drive the process. Turgor pressure is a pressure set-up within a cell due to the process of osmosis where uptake of water into the cell takes place across a semi-permeable membrane. This occurs due to the cells having a lower (more negative) osmotic potential than the environment surrounding them, which in turn creates a water concentration gradient and water influx. This increases the volume of the protoplast and will push the PM against the cell wall in walled organisms such as bacteria, fungi, plants, and oomycetes. The protoplast is said to be in a turgid state when turgor is generated within the cell. Thus, organisms which possess cell walls are known to have turgor pressure, whereas organisms which only have a cell membrane lack this pressure since the forces exerted by it could lead to cell lysis (Lew, 2011). Studies have shown that hydrostatic pressures of up to 20 bars (2.0 MPa) can be exerted on microbial and plant cell walls (Money & Harold, 1992) and in extreme cases, for example in appressoria pressures of up to 80 bars has been recorded (Howard et al., 1991).

Biophysics of turgor

Turgor arises due to a complex interplay between pressure and volume, water flow and extensibility. Pressure, cell volume and solute concentration are related as shown by the Ideal Gas Law,

$PV = nRT$

(where P = pressure, V = volume, n = the number of moles of osmotically active solutes, R = the gas constant and T = temperature). Thus, if the volume increases as a cell grows, then both the solute concentration and pressure will decrease. This is suggested to be the function of an increasing modulus of elasticity due to pressure buildup within the cell and measuring hyphal diameters could predict the action of turgor pressure within the cell in some cases (Lew, 2011). Therefore, for continued growth, there needs to be an influx or synthesis of solutes. Depending on the hydraulic conductivity of the membrane this will then lead to the uptake of water, which acts to keep the pressure constant. For the cell to continually extend, a specific amount of turgor is required, a threshold value beyond which the tip of the cell will yield and the volume will increase (Figure 1.2).

But if the cell wall lacks extensibility the increase of either pressure, volume or water flow will lead to the bursting of the cell. Investigations have shown that in algae such as *Chara* and *Nitella* the cell extensibility is maintained by crosslinks formed between pectin and Ca^{2+}, while in oomycetes such as *A. bisexualis* and *Saprolegnia ferax* this role is suggested to be played by endoglucanases, which are thought to loosen up the cell wall allowing for turgor to drive the growth of the cell. (Lew, 2011; Money & Harold, 1993). However, it should be noted that this role of endoglucanases is not supported by the steady state model and hence might be debatable.

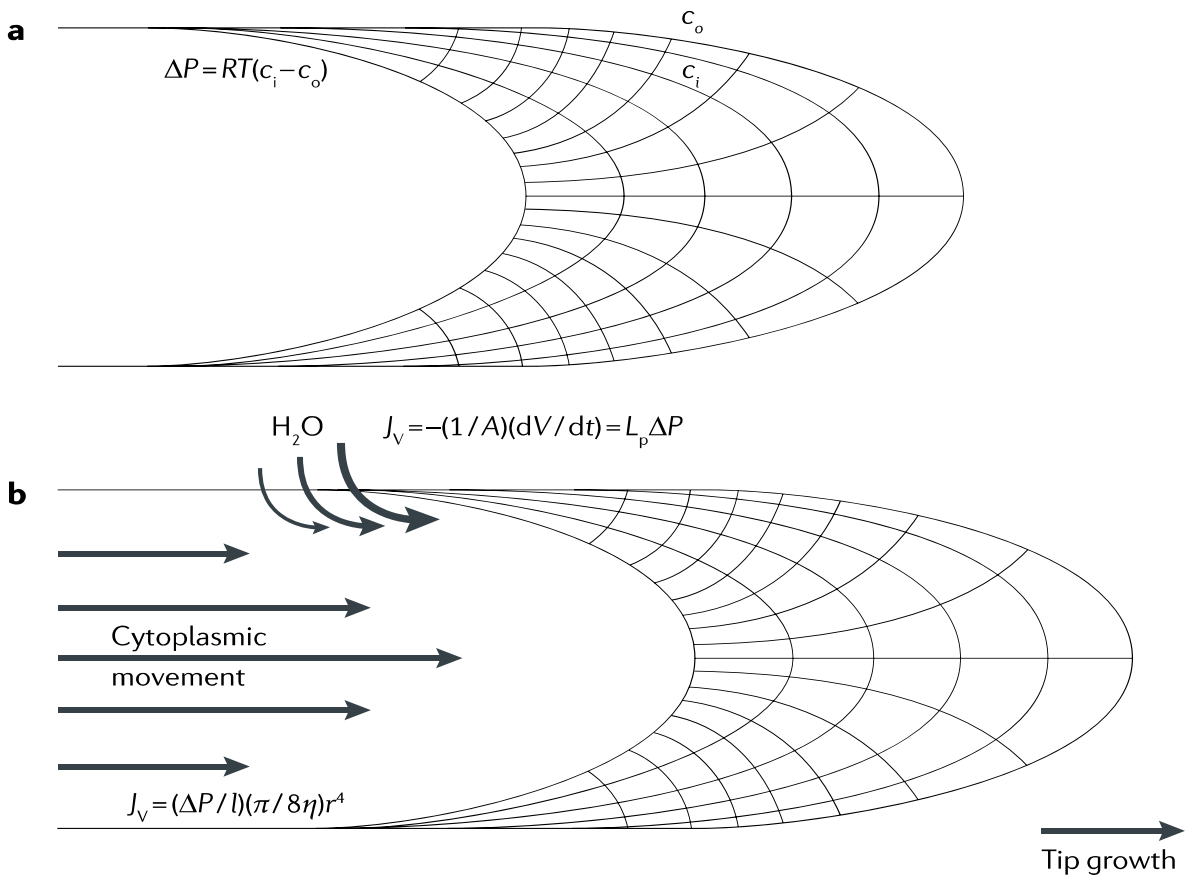

Figure 1.2: The relationship between pressure, volume, water flow and tip growth. The difference in solute concentration inside ci and outside co the cell lead to a pressure gradient across the membrane as shown by the equation in part (a). Water flow into the cell (curved arrows in part (b) is governed by this gradient and the hydraulic conductivity and also the volume change over time. Migration of the cytoplasm along with the growing tip could depend on the small intra-hyphal pressure difference that is created by tip expansion (straight arrows in part (b). Reproduced from Lew (2011) with permission.

1.10 Methods for studying turgor pressure

Turgor pressure can be measured either directly or indirectly, using a variety of techniques including thermocouple psychrometry, incipient plasmolysis, isotopic tracers, and single cell pressure probing (Muralidhar et al., 2016). Amongst these techniques the direct method of pressure probing is most reliable in measuring cell turgor. A single cell pressure probe consists of a glass microcapillary filled with oil, which is used to impale the cell (Cosgrove, Ortega, & Shropshire, 1987). This was initially designed to study turgor within plant cells, but was used on fungi for the first time in 1990 (Money, 1990). As the probe is inserted in a cell, turgor pressure causes some of the protoplast to push against the oil and move up into the capillary forming a characteristic meniscus. A motor is used to drive a steel rod down the capillary and this pushes the meniscus back down toward the cell. As the meniscus reaches the tip of the pipette the pressure that has been applied (which can be measured using a pressure transducer) is approximately equal to the turgor pressure of the cell (Money, 1990). Other methods include micromanipulation where turgor in spherical single cells can be measured. This technique involves the compression of a cell beneath a micromanipulation probe and the surface of a glass chamber, with the turgor measured using the pressure probe. The technique offers more stability while impaling of the cell is carried out. Results were comparative to those obtained from single cell pressure probing method (Wang et al., 2006). Another method compares the difference between the melting points of ice crystals (formed in fluid within the cell) and fluid surrounding the cell, where ice crystals are formed by maintaining the cell on a cold stage (Money & Howard, 1996). The results and conclusions of some of these studies are discussed below.

1.11 Turgor regulation

Since the hyphae extend into different environments, which inevitably would vary in osmotic concentrations, they need to maintain their internal turgor, especially if tip growth amongst other biological processes are dependent on it. To help with adjustments to these changes, cell walled organisms modify their internal osmotic potentials, which is a process called turgor regulation. To study this, external osmotic potentials can be altered with either impermeant or permeant osmolytes such as PEG, sucrose or sorbitol. Permeant osmolytes decrease internal pressure by releasing water from within the cell, after which they regain turgor if they can turgor regulate. In contrast, when impermeant osmolytes are used, the cell self regulates turgor by production of

their own osmolytes (Lew, 2011). While findings from fungal studies have suggested that they can turgor regulate, this does not appear to be the case for oomycetes. Single cell pressure probe experiments with *A. bisexualis* exposed to hyperosmotic shock suggest an inability to turgor regulate, this may also be the case with giant celled algae such as *Nitella* (Money & Harold, 1993).

Comparative measures of turgor between closely related oomycete species, *A. bisexualis* and *S. ferax* have been made in normal PYG media where turgor is typically around 0.6 MPa. However, when they were exposed to media supplemented with osmolytes giving external osmotic pressures that exceeded 0.70 and 0.50 MPa their internal turgor was below 0.02 MPa, below the measurable limit. Despite this hyphal extension in both species increased from 8 µm min^{-1}, in the absence of added osmolytes to 15 µm min^{-1} when these were added. The characteristic hyphal shape of *A. bisexualis* was lost and replaced by plasmodium like colonies at below measurable levels of turgor. In contrast, *S. ferax* maintained its hyphal shape - the reasons for such variation in structure is not known (Money & Harold, 1993). *A. bisexualis* was also unable to recover turgor after a hyperosmotic shock of 0.5 - 0.6 MPa, while with a hypoosmotic shock of 0.05 MPa it showed turgor regulation (although it should be noted that the application of a hypoosmotic shock is technically difficult due to the presence of ions in the agar).

In *S. ferax* linear growth rates continued to decrease, though there was an increase in osmotic pressure leading to a constant turgor within the cell. When K^+ channels (present in the protoplast) were inhibited by agonist, fluctuations of growth rates was observed but there was no substantial change in turgor within the cell. A positive correlation between turgor and growth rate was noticed for only hyphae, which grew above rates of 12 µm min^{-1}, however no change was noticed when turgor was constant (Kaminskyj, Garrill, & Heath, 1992). This was further strengthened by findings that *S. ferax* hyphae grew at faster rates when there was absence of measurable turgor (as indicated by pressure probe readings). However, these hyphae lost the ability to penetrate solid media and their tips were blunter. This was suggested to be the result of a more plastic tip, generated by the cell wall weakening by endoglucanases, thus causing the tip wall to remain fluid and extend easily (Harold, Money, & Harold, 1996). It could thus be suggested that there is an increase in growth rate even in the absence of turgor. This theory has been questioned by the fact that cell wall becomes weaker when exposed to osmolytes resulting

in the easy expansion of the cell under low turgor pressure (that is below the transducer reading point). If the cell wall remains rigid then higher turgor is required for tip extension. However, their loss of ability to invade host tissue suggests that turgor is necessary for invasive growth (Osiewacz, 2002).

In the case of *N. crassa* it was found that they could regulate turgor even after experiencing a hyperosmotic shock of 0.6 MPa and recovered within 100 minutes, while in the case of hypoosmotic shock of 0.31 MPa no turgor change was observed and hence it is proposed that they are able to self-regulate turgor (Lew et al., 2004).

1.12 Turgor studies in hyphae of fungi and oomycetes

Using the pressure probe method turgor has been measured in both fungi and oomycetes with reported values for *A. bisexualis* between 0.46 to 0.65 MPa (Money & Harold, 1992), 0.4 MPa for *S. ferax* (Money & Harold, 1992) , 0.2 to 0.48 MPa for *N. crassa* (Lew et al., 2004) and 0.1 MPa for *Morchella esculenta* (Amir et al., 1994). The turgor pressure in *N. crassa*, has also been measured throughout the length of the hyphae using the method of incipient plasmolysis. Pressures in the apical cells were 12.4 atmospheres (1.26 MPa), which increased in the basal cells to 17.5 atmospheres (1.77 MPa). These results correlated with those for the fungus *Fusarium oxysporum*, which also suggested that turgor pressure along a hypha was not uniform (Robertson & Rizvi, 1968).

1.13 Role of turgor in infectious apparatus

The appressorium in the rice blast pathogen, *Magnaporthe grisea*, is thought to help with penetration of host tissue by the buildup of turgor pressure within the cell. As the tips of appressoria are fragile turgor pressure studies have had to use an indirect method of testing, due to the possibility of rupturing the cell upon insertion of a pressure probe. Turgor pressure in these infection structures can be measured by estimating the force required during penetration of host. In these investigations host substrates can be mimicked using different synthetic substrates with varying surface hardness, for example polyvinyl chloride or a range of Mylar membranes. The latter, are nonbiodegradable and can be developed in a wide range of surface hardness's, which may possibly replicate the resistance of the host tissue. The turgor measured in these cells was found to be proportional to surface hardness of the substrate. Small changes in turgor meant that

the hardest membranes became impenetrable, while a larger change in turgor pressure was required for softer membranes to be rendered impenetrable (Howard et al., 1991). While this might suggest that turgor pressure plays a crucial role in host penetration, strains that carried mutations of the mitogen activated protein kinase genes *mps1* and *pmk 1* were unable to penetrate the hosts (Xu & Hamer, 1996; Xu, Staiger, & Hamer, 1998). Studies on pollen tubes, and various other plant and animal cells suggest that when cells are osmotically stressed they produce increased levels of signaling lipids such as phosphotidic acid causing the activation of signaling pathways, including MAPK pathways, which are suggested to be involved in maintenance of turgor pressure and this might explain the role of these genes in maintaining turgor (Munnik & Vermeer, 2010).

Other roles of turgor

In addition to driving tip growth, turgor is also thought to power spore dispersal in *Ascobolus immerses*. These organisms produce up to 8 spores, which are expelled simultaneously. Pressure probe readings have measured a total pressure of 0.3 MPa within these cells, out of which 0.1 MPa pressure was generated in the ascus cap. Mathematical modelling of these pressures in the organism, suggested that 0.2 MPa, which is in the cell is sufficient for spore dispersal (Fischer et al., 2004).

Another key role of turgor pressure is thought to be its association with mass flow, which has been investigated in both fungi and oomycetes and has been proposed to play a role in tip growth (Lew, 2005; Muralidhar et al., 2016).

1.14 Mass flow

The principle of mass flow has been associated with the movement of water, sap and gases within higher plants for several centuries. According to this, there is the bulk movement of material down to an area with lower pressure upon the establishment of a pressure/temperature gradient. Evidence from several studies in filamentous microorganisms has suggested that this same principle might be associated with various roles in them, including the movement of the cytoplasm, organelle transport, movement of nutrients to the growing tip and polarized tip growth (Angeles et al., 2004; J. M. Baker & van Bavel, 1987; Lew, 2005; Muralidhar et al., 2016).

1.15 Mass flow in plants

Higher plants require long distance transport of essential components for growth such as water, nutrients and carbohydrates, which are supplied by two primary systems, the xylem and phloem. Nutrients from the soil are transported to the leaves via the xylem, while phloem supplies products such as amino acids and electrolytes from the leaves to various plant tissues. Transport within both systems is suggested to be the result of establishment of a pressure gradient which is explained by such theories as, Cohesion theory (proposed for the xylem) and the Münch hypothesis (proposed for phloem) (Dixon & Joly, 1894; Munch, 1930). According to the Cohesion theory, pressure gradients within the xylem are established due to evaporation on the surface of leaves resulting in increased surface tensions. The entire plant is affected by the transfer of this tension, starting at the rigid cells of the xylem and the root apices (Angeles et al., 2004). The pressure flow hypothesis (Münch hypothesis) of phloem suggests that a pressure gradient is established by the loading of osmotically active solutes such as sucrose at the leaves (source), and its removal and transfer from the sap (sink) to the tissues of the plant. (Ziegler, 1975).

1.16 Methods of studying mass flow in plants

Testing the validity of these theories in a living system have proved problematic due to the techniques employed in studying these delicate structures. Xylem is deeply embedded within the plant and operates under tension, even slight damage due to cutting and puncturing could easily injure them (Wei, Tyree, & Steudle, 1999). Living cells in the phloem mount defense

mechanisms even under the slightest invasive manipulation (Knoblauch et al., 2001; Van Bel, 2003). Thus, several techniques have been trialed including molecular techniques, pressure probing, non-invasive heat techniques and radioisotope labelling. Each technique has its own drawback, for example: though pressure probe produces more accurate turgor pressure readings, they are invasive and hence cause damage (Gould, Minchin, & Thorpe, 2004; Tomos & Leigh, 1999). Radioisotope labelling might require destruction of sampled tissue and measures the carbon flow rates rather than the water flow rate, which might result in inaccurate readings (MacRobbie, 1971; Minchin & Thorpe, 2003). The heat techniques could be invasive if there is requirement of inserting a probe within the plant, however some modifications in heat techniques allow for external establishment of temperature gradients using gauges (D. Smith & Allen, 1996).

About a decade ago, the introduction of nuclear magnetic resonance imaging (NMR) provided a non-invasive technique of studying mass flow rates within both xylem and phloem. By 1988, imaging techniques were added to NMR (Van As & Schaafsma, 1984). However, it was first used in a living system to test flow rates in the xylem in 1997, within a seedling of castor bean (6-day old) (Köckenberger et al., 1997). A faster system called FLASH was eventually developed which could measure xylem velocities in a 40-day old castor bean (Rokitta et al., 1999).

However, in the case of phloem flow rate studies, even NMR has found little success mainly due to the small flow volumes of phloem sap. A modified NMR technique has shown promising results in measuring sap velocities in both xylem and phloem, and has compared the flow velocities in four plants namely, tomato, poplar, tobacco and castor bean (Windt et al., 2006).

1.17 Mass flow in filamentous microorganisms

It has been suggested that mycelia of tip growing organisms behave like micro-hydraulic networks, where the flow of cytoplasm can be compared to movement of water flowing within a circular pipe (Figure 1.3) (Lew, 2011). As mentioned earlier there was a noticeable difference in the pressures measured at the base and tip of *N. crassa*, and this finding strengthened the theory that movement of cytoplasm could be due to turgor driven mass flow when pressure gradients as low as 0.05-10 kPa cm^{-1} are present (Lew et al., 2004).

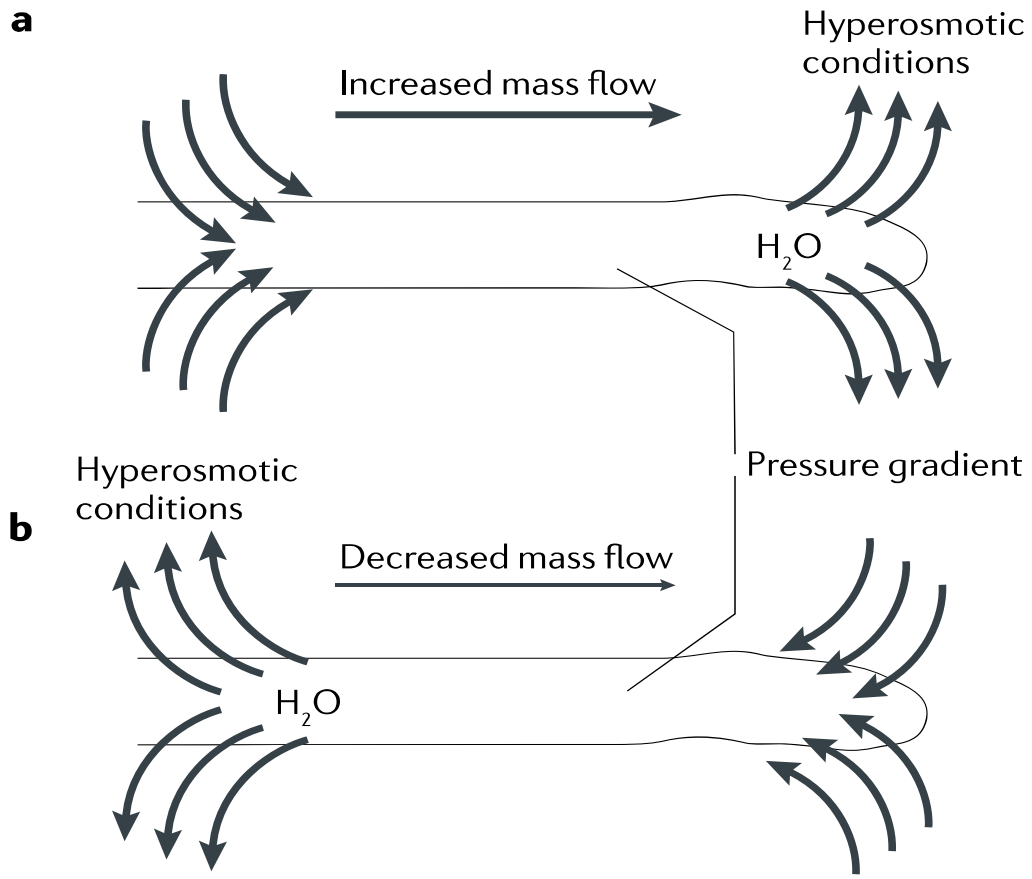

Figure 1.3: Mass flow of the hyphal cytoplasm as shown in experiments on single hyphae of the fungus *Neurospora crassa*. A change in the pressure gradient in the hyphae by the localized application of hyper- or hypoosmotic solutions causes the movement of water as shown by the curved arrows. a) Efflux of water at the tip leads to mass flow b) Efflux of water subapically reduces the mass flow. Reproduced from Lew (2011) with permission.

1.18 Methods of studying mass flow in filamentous microorganisms

During the development of *M. esculenta* sclerotia a difference in turgor pressure between mycelium and the growing sclerotia was observed (Amir et al., 1992; Amir et al., 1994). They were grown on a split petri-dish consisting of defined media on one side with water potential of 0.5 MPa and Nobel agar supplemented with glucose on the other, with water potential of 2.1 MPa. Data suggests that during sclerotial development the pressure gradients between the mycelium and sclerotia reached 0.53 MPa, which resulted in the increase of turgor pressure. During specific stages of development, a change in pressure was registered, especially during branch formation on the sclerotial side and growth of hyphae towards the mycelial edge. These results were consistent with observations during an earlier study to map translocation using radiolabeled molecules. [^{14}C] 3-O-methyl glucose and [^{14}C] D-glucose translocation between the mycelium side to the developing sclerotia followed a similar pattern (Amir et al., 1994). It could be suggested that the mycelium act as sources, absorbing nutrients from the medium to supply the rapidly developing sclerotia (sinks). To achieve this a low pressure needs to exist in the primary hyphae, to draw mass flow. However, the sclerotial tissue at the edge would have to have high turgor pressure to drive cell expansion (Amir et al., 1994). It should be noted that turgor was measured using a direct method within the mycelia, while indirect measurements were obtained from the growing sclerotia, which was too small for direct measurements. It has been suggested that the change in turgor would correspond to the movement of nutrients by turgor driven mass flow towards the growing edges of the organism (Amir et al., 1994).

While the presence of a gradient due to different turgor pressures could enable mass flow, to actually observe mass flow, material with sufficient contrast would have to be introduced into the cell. It would not be sufficient to simply measure movements of organelles inside the cell because as previously mentioned cytoskeletal elements within the organism also participate in the movement of cellular contents within the hyphae. With this in mind, low-viscosity oil droplets have been injected into *N. crassa* hyphae using a single cell pressure probe and have been used to measure mass flow in *N. crassa* hyphae. The silicone oil droplets were injected into the hyphae using a pressure probe apparatus. Although, this is similar to studying turgor pressure using pressure probe, a larger force is applied to actually inject the oil droplet into the cell. Upon establishment of a pressure gradient by addition of osmotic solutions, any movement of the oil

droplet can be observed. The use of a silicone oil droplet means that movements should occur independent of the movements of molecular motors along cytoskeletal tracks as these should not bind to the oil. Observations have shown oil droplets in *N. crassa* hyphae to move towards areas that were lower in pressure (Lew 2005). This suggested that mass flow might contribute in tip growth of these organisms even though only modest pressure gradients were observed (Lew, 2005).

Similar studies have yet to be carried out on individual oomycete hyphae. Movement of oil has been observed in hyphae when pressure gradients were set up across mycelia of *A. bisexualis* and the rate of movement was consistent with a possible role in tip growth, facilitating the bulk movement of the cytoplasm forward as the tip extends (Muralidhar et al., 2016). In these experiments single spores were inoculated onto split petri-dishes with media containing 0.3 M and 0 M sorbitol on each side of the dish. As the zoospore germinated it formed a mycelium, which grew on both sides of the dish. The inability of *A. bisexualis* to turgor regulate meant that the difference in media set up a turgor gradient across the dish. The direction and rates of oil droplet movement were as predicted by the gradient and the Hagen-Poiseuille equation (see below) with rates of 1.8 ± 0.46 μm s^{-1} during anterograde movement as compared to 1.8 ± 0.37 μm s^{-1} on the 0 M and 0.3 M side, while retrograde rates of 1.6 ± 0.65 μm s^{-1} and 2 ± 0.40 μm s^{-1} were observed, respectively (Muralidhar et al., 2016).

1.19 Hagen-Poiseuille equation

According to microfluidics, if flow within the hyphae resembles flow through a pipe, it should be laminar rather than turbulent. In *N. crassa*, the Reynold's number was calculated using the equation

$Re = (\rho \upsilon d) / \eta$ [ρ – the density, υ – velocity of flow, d – tube diameter and η – viscosity].

This calculated value (10^{-4}) suggests that the flow is laminar ($Re < 10^{-3}$) (Lew, 2005). To the best of our knowledge this value is not known for oomycetes but the similarities observed within fungal and oomycete hyphae suggest that laminar flow could occur within them and the Hagen-Poiseuille equation used for theoretical flow rates. In the mycelia of *A. bisexualis* this theocratical rate was noted to be10 times slower than the observed rates. (Lew, 2011; Muralidhar et al., 2016).

1.20 Lab-on-a-chip technology

The distinguishing character of Lab-on-a-Chip devices are their ability to effectively create a miniature laboratory on a small chip (Agudelo et al., 2013). Recently this technology was employed to analyze forces and modes of growth of different microorganisms. Measurements can be generated at the micro-nanoscale by designing transducers based on microelectromechanical systems (MEMS), which creates a superior designing system for measurement of internal forces, while being non-invasive, cost effective and flexible. Complex computational calculations are not required for chip development, which makes them easily accessible for biological studies (Halldorsson et al., 2015).

Drawbacks

These devices (chips) are silicone-based, which could have several drawbacks during processing, biocompatibility, aqueous environment exposure and microfabrication (Johari et al., 2013). For the measurement of cellular traction forces, post/pillar structures are developed from polydimethylsiloxane (PDMS), an inert, biocompatible, transparent, non-toxic and non-flammable silicone oil. Cells are normally grown in sufficient media in culture flasks, plates etc., hence their growth on PDMS chips requires specific protocols to reduce hydrophobicity and supply nourishment to the organism (Johari et al., 2013).

1.21 Some studies using LOC devices

LOC devices have been used to measure forces of locomotion in *C. elegans*, growth of pollen tube and measurement of growth forces in fungi and oomycetes. These PDMS chips used in *C. elegans*, fungi and oomycetes, were fabricated to enable the growth and/or movement of the organisms within a matrix of micropillars that were located in channels. The pillars were displaced as the organisms grew or moved into them and the degree of displacement could be converted into a measurable force. A force of 55.41 µN was for example measured for a young adult wild-type *C. elegans* (Ghanbari et al., 2012; Johari et al., 2013). Similarly, TipChip technology has been used to investigate the forces generated by pollen tubes by designing micro-channels that mimicked *in vivo* growth environment and these enabled the testing of the dilating force involved in penetrating tubes with the physical properties of PDMS (Agudelo et al., 2013).

The Lab-on-a-chip method has enabled the measurement of protrusive forces generated by *A. bisexualis* (Tayagui et al., 2017) and the hyphae were shown to be able to grow on the chip devices. In view of this, in the research described in this thesis, I have designed and used chip devices with the aim of streamlining the process of studying mass flow within a single hypha. While mass flow of gases has been successfully studied using Lab-on-a-chip technology by changing pressure gradients within the micro-channels (Arkilic, Breuer, & Schmidt, 2001; Ewart et al., 2007; Yoon & Wise, 1992), to the best of my knowledge such studies have not been undertaken for fungal or oomycete mass flow. This led to the design of chips where the organism grows and it is possible to isolate a single hypha, allowing the microinjection of silicone oil into the cell and the change of the external pressure gradients and to observe any mass flow.

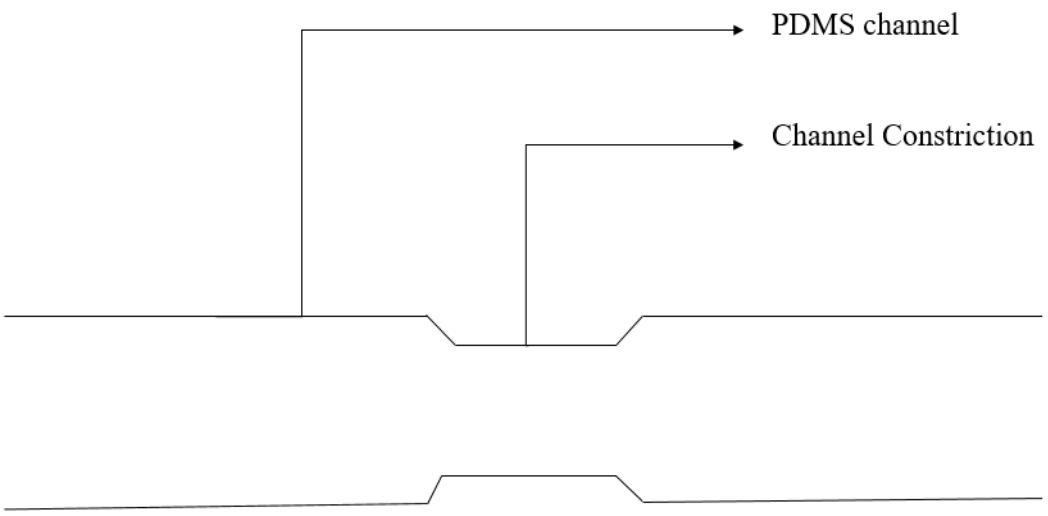

Figure 1.4: Design of single micro-channel of the inverted chips designed to carry out mass flow study. The micro-channel dimensions are, 35 µm in width, 3 mm in length and constriction in the middle 25 µm wide.

1.22 Hypothesis

- Mass flow will occur within a single hypha of the oomycete *A. bisexualis*
- Oil droplets will move in the direction predicted by an imposed pressure gradient
- The rate of droplet movement will be the same as that predicted by the Hagen-Poiseuille equation
- Microfluidic devices will allow the microinjection of silicone oil into hyphae

Chapter 2. Materials and Methods

2.1 Stock Culture and maintenance

A female strain of *Achlya bisexualis* Cocker, which had been previously isolated from the dung of *Xenopus* and held in the University of Canterbury culture collection, was used for all experiments in this thesis. *A. bisexualis* was sub-cultured onto 2% peptone-yeast-glucose media containing in gL^{-1}; glucose 3 (Sigma Aldrich Chemicals Pvt. Ltd, India), bacteriological peptone 1.25 (Oxoid Ltd., England), yeast extract 1.25 (Oxoid Ltd., England), and bacteriological agar 20 (Oxoid Ltd., UK) made up with distilled water. The media was then autoclaved and plates were prepared by pouring PYG into 85 mm diameter petri-dishes in the sterile environment of the LAF hood and allowed to set. These plates were stored at 4^0C prior to their inoculation.

The process of sub-culturing was carried out weekly using plugs cut with a 5 mm core borer from the edge of the growing colony and placed onto PYG plates using a sterile scalpel and then sealed using parafilm. The inoculated petri-dishes were kept at room temperature in the dark.

2.2 Experimental cultures

Mass flow experiments were carried out on cultures grown in 55 mm diameter petri-dishes, containing approximately 3 mL of 2% PYG. Plugs were cut using a 5 mm core borer from the growing edge of a stock culture to inoculate the plates. They were then sealed with parafilm and kept at room temperature in the dark. The mass flow trials were carried out 48 to 72 hrs after inoculation with *A. bisexualis* on the petri-dish.

2.3 Mass flow experiments on a petri-dish

To investigate whether mass flow can occur in *A. bisexualis* hyphae, silicone oil droplets were injected into a single hypha using borosilicate microcapillary pipettes. All experiments were carried out under the 10 X objective lens of an inverted Zeiss IM 35 microscope, West Germany. All data during this thesis was documented using a USB 3.0, xiQ, Ximea camera.

Previous studies on mass flow via invasive techniques have used a pressure probe apparatus to microinject silicone oil into the hyphae (Lew, 2005; Muralidhar et al., 2016). For this thesis, a new custom designed system was developed. This comprised a linear syringe pump that consisted of a 5 mL plastic syringe attached to a stand with a plastic bracket. The plastic plunger of the syringe was replaced with a metal plunger, the upper end of which was fitted to a large

metallic screw. The syringe was powered by a circular, hand controlled syringe pump motor speed controller.

The syringe was filled with low viscosity silicone oil (approximately 3 to 4 mL), either by using the motor attached to medical grade polyethylene tubing or by pouring the oil from a vial into the inverted syringe. All air bubbles were eliminated from the syringe by purging.

Initially, the hub of the syringe was connected to a metallic screw connector, to which medical grade polyethylene tubing was attached. The other end of the tubing was then attached to a brass pipette holder into which the pulled borosilicate glass pipettes of different diameters were fitted. A rubber O-ring was used to seal the pipette into the holder. The pipette holder was attached to micromanipulators. A STM-3 joystick was attached to these micromanipulators and helped control the movement of the holder and glass pipette along X and Y-axes.

However, due to the pressure generated by the syringe and lack of adequate resistance, there was some leakage of the oil from the end of the brass holder. Hence, to offer more resistance to oil leakage, the following modifications were made.

Firstly, the hub of the syringe was attached to a P-628 luer adapter, fitted into a XP- 235x flangeless fitting with a standard P200x ferrule within it. One terminal edge of ETFE (ethylene-tetrafluroethylene) tubing with an inner diameter (I.D.) of 0.50 mm and an outer diameter (O.D.) of 1.59 mm was inserted into the flangeless fitting. The other end of this tubing was connected to a P-702 low pressure union containing a standard P200x ferrule (all from IDEX, Health and Science). The union was held in place on the micromanipulator stand by a screw with a brass holder attached to the end of the union. The brass holder was then mounted onto the micromanipulator stand. The pulled glass pipettes were inserted into the ferrule of the low-pressure union and this created a continuum between the tubing and the glass pipette. With these modifications there was little to no leakage of oil when the pipette tip was inserted into hyphae and positive pressure applied. The set-up is shown in Figure 2.1.

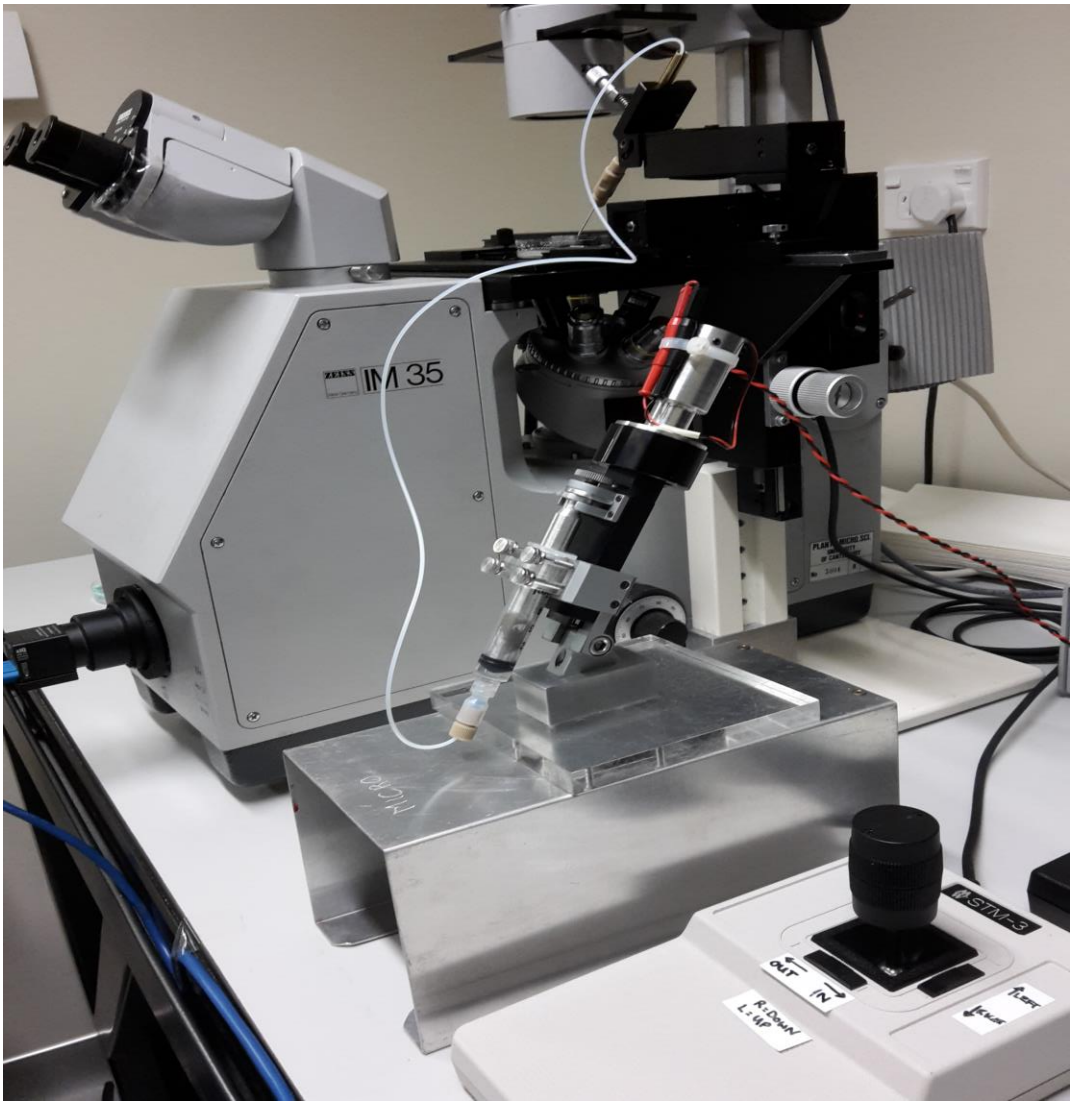

Figure 2.1: Microinjection set up - This includes a linear syringe pump attached to a stand of micromanipulators, connected by ETFE tubing. The joystick allows for alignment of the brass holder along with its attachments holding the glass micropipette in place. The entire process is carried out under an inverted Zeiss IM 35 microscope.

2.4 Pipette puller

A Narishige PC-10 model pipette puller was used to produce glass micropipettes from borosilicate glass microcapillaries. The borosilicate glass capillaries used had dimensions of 1.5 mm O.D. x 1.17 mm I.D. or 1.5 mm O.D. x 0.86 mm I.D., (Harvard Apparatus, Kent, England). The latter capillaries were used as the manufacture of the former was discontinued and so these were unavailable. Irrespective of which capillaries, before the pipettes were pulled, both ends of the glass capillary were fire polished using the flame of a Bunsen burner for 5 s and allowed to cool. This ensured that the end of the capillary was smooth, which helped retain the integrity of the O-ring and ferrule when the pulled pipette was inserted into the pipette holder. The end of the capillary was rotated during the fire polishing process to ensure equal polishing around the rim.

The glass pipettes were produced using the single pull setting on the pipette puller (Figure 2.2). The pipette puller uses different voltages passing through its coil, which corresponds to different temperatures at which the pipette is pulled.

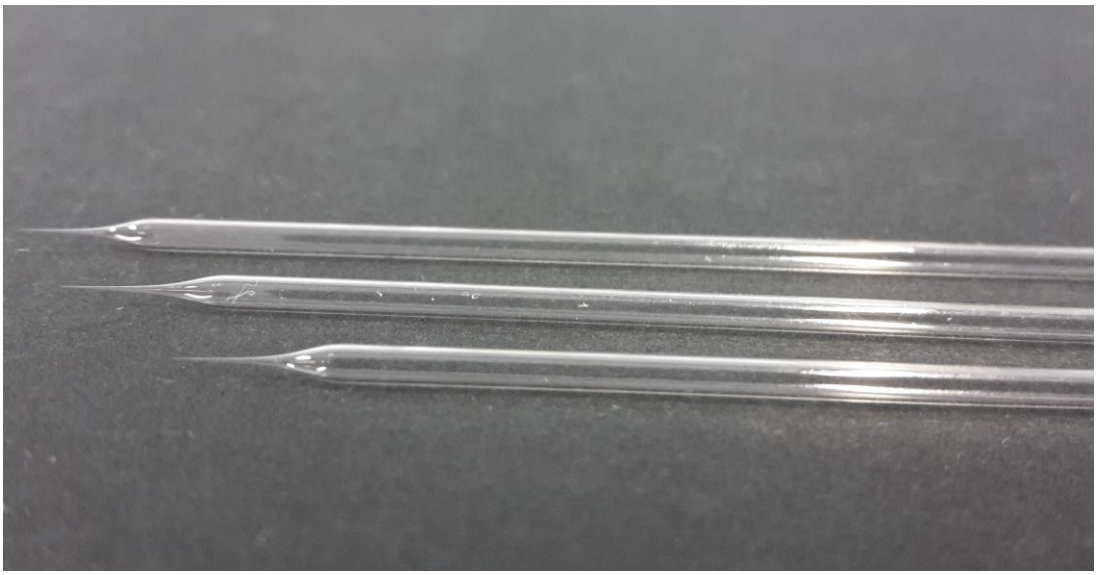

Figure 2.2: Borosilicate glass micropipettes pulled using the single pull of the pipette puller at 64 VU. These are filled with silicone oil before being used for microinjection of the hyphae.

Initially, the entire glass pipette was filled with low viscosity silicone oil, this was done using 1 mL plastic syringes that had had their tips stretched after placing into a Bunsen flame such that the tip was then able to reach down to the end of one of the pulled pipettes. If an air bubble was observed at the tip of the pipette it was eliminated by tapping it several times. Another technique that was trialed was to attach the pipette to the pipette holder and to fill it using the syringe. The oil from the syringe pump was pumped into the glass pipette, while it was held vertically to avoid the formation of air bubbles. Unfortunately, this method led to leaking or breaking of the glass tip in most cases and hence it was discontinued. The failure of this method could be due to the pressure exerted by the pump. Therefore, to control the amount of oil, which was to be injected into the hypha the experiments were run by filling the glass pipette with approximately 1 to 2 cm of silicone oil using the 1 mL plastic pulled syringe and lightly tapping to eliminate any air bubble at the tip of the pipette.

It was very difficult to control the exact pressure required to insert the silicone oil into the hypha. Changes had to be very delicate, in many cases there was extra release of oil within the hyphae, causing it to burst. Several attempts lead to a very strong wound response, which was generated by the movement of vesicles within the cell towards the invading pipette. This caused the blocking of the pipette on several occasions and in these instances the recordings had to be discarded. In a couple of cases oil droplets within a cell were pressurized out of the cell through unsealed wound sites.

To carry out the mass flow experiments the petri-dishes were unsealed and placed on an inverted Zeiss IM 35 microscope. The pipette was adjusted to the optimal angle and area of the mycelia for impaling a single hypha under the 4 X objective. The process of injecting and observation of oil movement was carried out under a 10 X objective. The set-up for injecting hypha on petri-dish is represented in Figure 2.3.

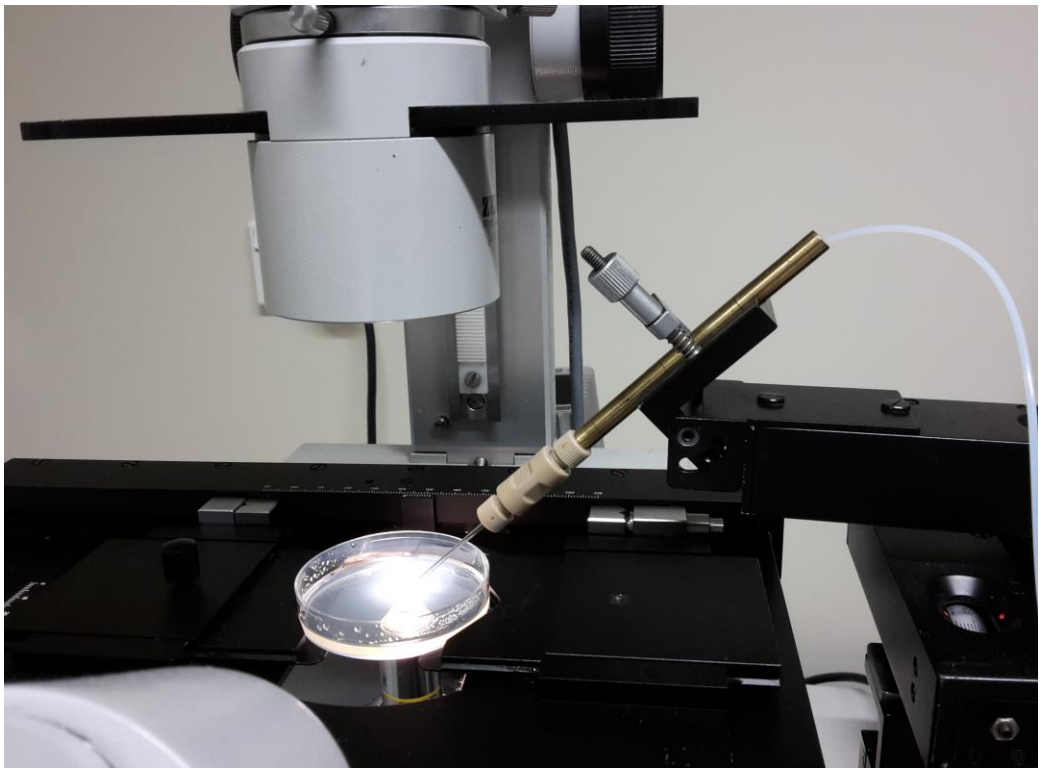

Figure 2.3: The set up for injecting oil within a hypha in petri-dish environment under 10 X objective lens of an inverted microscope. The micropipette is initially aligned with the hypha in the agar under 4 X objective lens, after which microinjection of silicone oil is carried out under the 10 X objective lens.

2.5 Osmotic treatment

The imposition of an osmotic gradient for these experiments was achieved by adding, in the case of hypoosmotic treatment, distilled water (20 µL) using a micropipette. The water was added at a distance of approximately one cm from impalement site. The distilled water was added either at the mycelium end or hyphal tip end. For a hyperosmotic shock 0.5 M sorbitol (20 µL) (Sigma, USA) was added at the mycelium end at approximately one cm from the impalement site.

Osmolality

To check the osmolality of PYG broth and the 0.25 M, 0.5 M and 1 M sorbitol solutions a vapor pressure osmometer (Wescor Inc., USA) was used. The osmolality of all 4 solutions are listed in Table 2.1.

Table 2.1: Osmolality of PYG and sorbitol solutions using vapor pressure osmometer

Solutions (concentration)	Osmolality (average ± SEM)
PYG broth	23.3 ± 1.2 mmol/kg or mOsml/kg
1 M sorbitol	1013 ± 2 mmol/kg or mOsml/kg
0.5 M sorbitol	491 ± 2.5 mmol/kg or mOsml/kg
0.25 M sorbitol	245 ± 1.3 mmol/kg or mOsml/kg

2.6 Poly-di-methyl siloxane chips

The PDMS chips were prepared at the nanolaboratory, Department of Engineering using the following protocol stated here in brief. For the process of fabrication, a replica-molding of a photoresist master was employed. Laser mask writer, (uPG101, Heidelberg Instruments), which contained the channel outlines and ports, this was used to prepare a 4" chrome on-glass photomask (Nanofilm). Using a hot roll laminator (SKY335R6, Sky-Dsb Co. Ltd) a 30 μm thick negative-tone resist (ADEX30, DJ Devcorp) was laminated onto a clean 4″ silicon wafer. At a speed setting of 1 and temperature of 65^0C lamination was carried out. In vacuum contact mode, the mask was then exposed into the ADEX30 layer using a mask aligner (MA-6, Suss MicroTec). Baking was then carried out for 5 min at 65^0C and 10 min at 95^0C on a contact hotplate (HP30, Torrey Pines Scientific, Inc.) followed by the use of the mask aligner. Using propylene glycol monomethyl ether acetate the wafer was developed and then rinsed with IPA. Drying was carried out using nitrogen gas.

The next step involved treating PDMS, which was used to cast the mold with trichloro (1H,1H,2H,2H perfluorooctyl) silane (SigmaAldrich) for 2 hrs. The process was carried out in a vacuum to facilitate the release of these molds. PDMS (Sylgard 184, Dow Corning) was mixed at 10:1 w/w ratio, degassed and poured onto the mold. Baking was carried out for 2 hrs at 80^0C, and after the cured PDMS was peeled off the mold, it was further baked for an additional 4 hrs at 80^0C to ensure hardening. Seeding area holes of dimensions 2 mm or 2.5 mm and inlet ports were punched into the PDMS at this stage. Cleaning of glass chip covers (standard 75 × 25 mm glass microscope slides, VWR) was carried out using acetone, methanol and IPA each for a time frame of 5 min, respectively. Using the barrel asher (K1050X, Emitech) both glass and PDMS were exposed to 100 W oxygen plasma, which was exposed for 30 s each and then bonded. The process of bonding was completed by a further bake of 2 hrs at 80^0C on a hotplate. Degassing was carried out for 2 hrs by placing the chips in a vacuum chamber. This helped in vacuum-assisted filling. Vacuum sealer (Sunbeam FoodSaver) was used to seal the degassed chips into food-grade vacuum bags and stored until use (Tayagui et al., 2017).

2.7 Chip Design

The PDMS chips were brought from the nanolaboratory, Department of Engineering, University of Canterbury, in air tight, sealed packets to the Department of Biology. Due to our experimental needs inverted chips were designed and used during this thesis.

The chips consisted of either glass slide, cover slip or Fluro dish as the base. The PDMS chips were bonded on either of these bases for the growth rate experiments. All the mass flow trials were carried out on chips bonded to glass slides. The chips were designed with two 2 mm wide circular seeding areas, parallel to each other and connected to two channels running across the length of the PDMS (Figure 2.6). The channel width was either 35 µm or 50 µm, while channel length varied from 1 mm to 3 mm and the channel height was 30 µm. The exit area of these channels was 2 mm in width. In some chips, a constriction of 25 µm width was created midway down the channels to allow the growth of a single hypha along the channel. Five sets of microchips were produced with slight modifications each time to optimize the growth of individual hypha down the chips.

Chip design 1

The first set of chips had the same basic design and dimensions as described above, but they were devoid of the exit area (Figure 2.4). To introduce PYG broth, these chips contained inlet ports on either side of the PDMS layer, which were further connected to the channels. To introduce broth in these chips, a 1 mL syringe containing the broth, [which had been checked to ensure that there were no air bubbles in it] was attached to ETFE (ethylene–tetrafluroethylene) tubing with I.D.–0.50 mm and O.D.- 1.59 mm and was inserted into the inlet ports of the channel. Broth was introduced by pushing the plunger of the syringe. To check if the channels were filled with broth they were observed under an inverted Zeiss IM 35 microscope. They were then taken to the hood for inoculation.

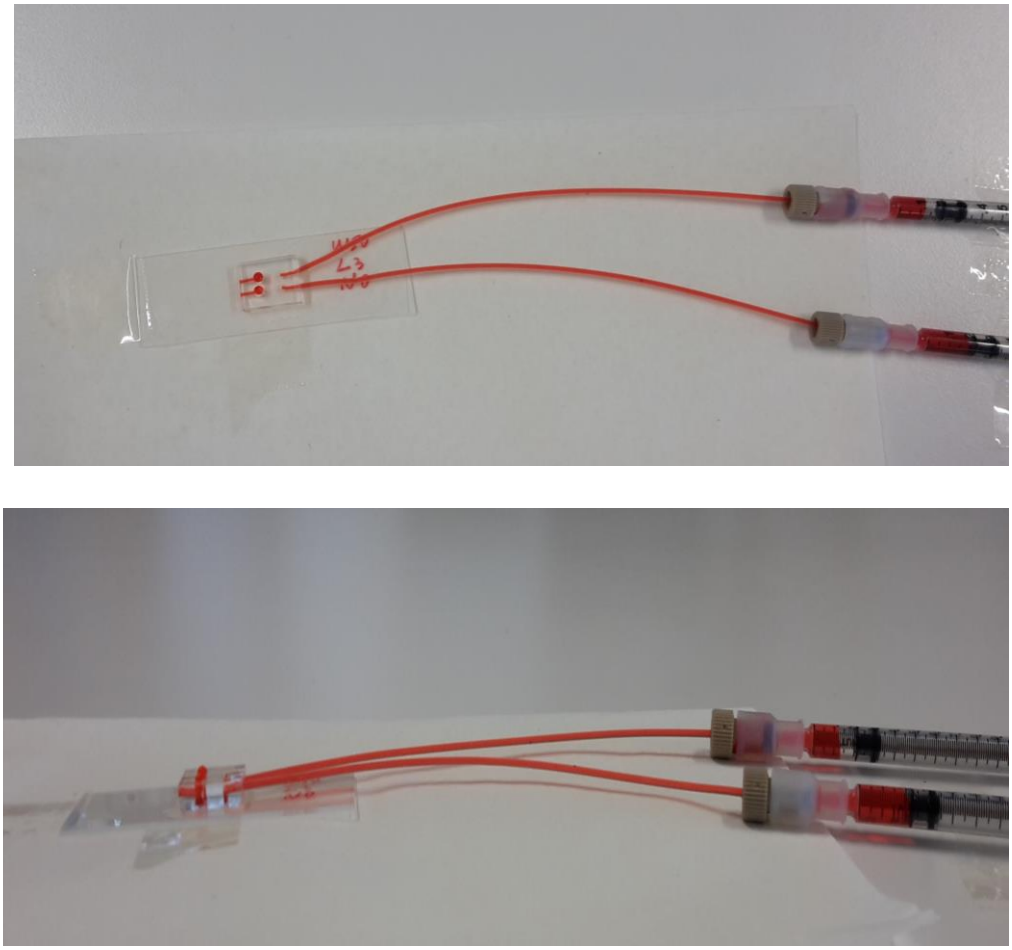

Figure 2.4: Chip design 1: Overview & Sideview-These PDMS chips were fitted with to two plastic 1 mL syringes filled with red dye. This was connected with plastic tubing into the inlet ports used for feeding of broth. The PDMS holes with red dye represent the seeding areas, which connected to the PDMS channels as represented by the red lines of the dye. The side view shows the PDMS chip layer which is bonded onto a glass slide.

Chip design 2

The second set of chips had the same basic design as described above but they lacked the inlet ports. The PYG broth was added into the seeding area using a 20 µL micropipette. Once broth was introduced into the chips they were then observed under the inverted microscope.

Chip design 3

The design of chip set 3 was the same as the previous set of chips in dimension and design except they were degassed for longer, 3:30 hrs as compared to the half hr of degassing normally done, to check if it would help with the flowing of the PYG broth through the PDMS channels.

Chip design 4

The fourth set of chips had the same dimensions and basic design as described above, but the PDMS layer was cut in various shapes to allow for access of the glass pipette for microinjecting the cells (Figure 2.5).

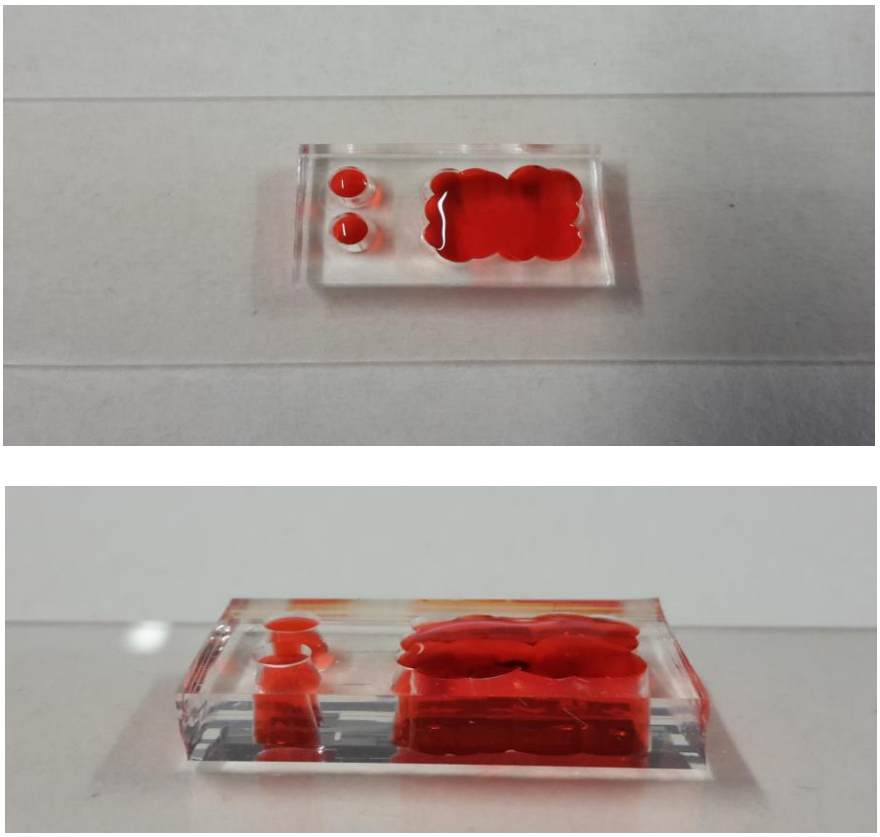

Figure 2.5: Chip design 4 – Overview & Sideview. These chips had the same PDMS channel design but large blocks of PDMS were cut out at the exit area. This was done to allow for the micropipette to be placed with ease near the hyphae during microinjection. The small circular holes are the seeding areas. The red dye fills in the exit area as well as the seeding area. But the PDMS channels were blocked in these chips and so the dye could not flow down. The side view shows the layer of PDMS chip bonded on a glass cover slide.

Chip design 5: These chips had the same dimensions as described in the basic chip design. Their seeding areas were enlarged to 2.5 mm to help with the flow of broth down the channels (Figure 2.6). The exit area was extended into large PDMS squares which were cut out to help getting the pipette aligned with the hyphae for microinjection (not shown). The PDMS layer was made thinner to help insert the pipette for microinjection and to reduce optical distortion.

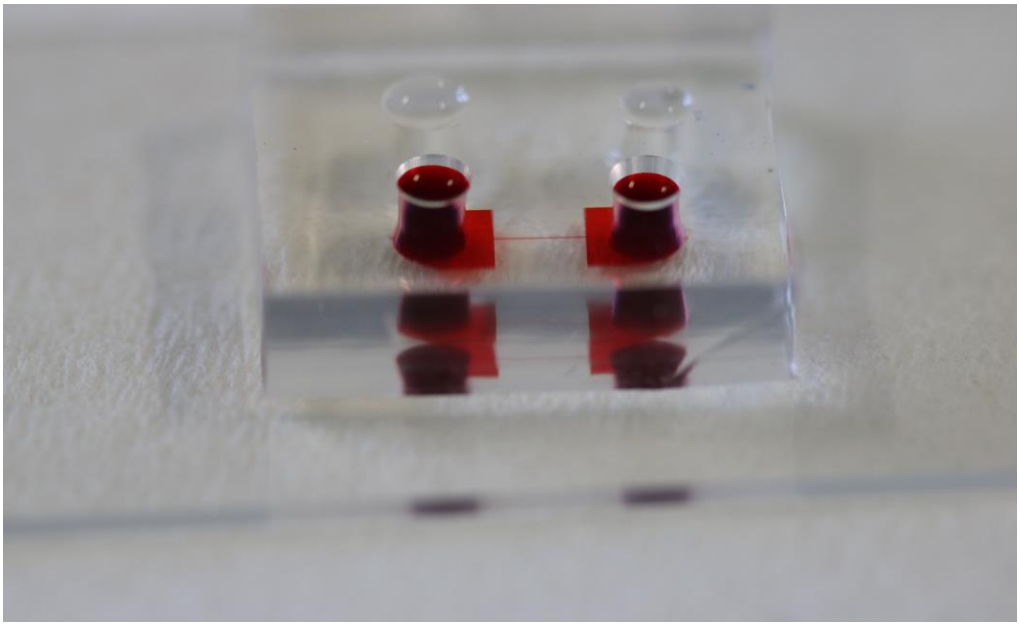

Figure 2.6: Chip Design 5- These chips have the same PDMS channel design but the PDMS layer was made thinner. The two circular holes opposite to each other represent a seeding area and exit area on the chip. Red dye flows down the channels of these chips showing the channel design. The parallel channel is filled with colorless PYG broth.

2. 8 Chip inoculation

In the sterile environment of the LAF hood, the sealed packets containing the chips were cut open and PYG broth, which was previously prepared and kept at 4^0C, was immediately introduced into the chips to avoid air bubbles. A 2 mm biopsy punch was used to cut a plug from the growing edge of the 48 hrs old culture, which was maintained in 2% PYG at room temperature. The plug was removed using a scalpel and inverted before placing in the seeding area. The inoculated chip was then placed in the dark and allowed to acclimatize after, which experiments were carried out with the chip on the stage of the inverted microscope. Growth rates were measured once hyphae entered the channels. When the hyphae exited the channel, attempts were made to microinject oil into the hyphae. Unfortunately, due to the flexibility of the hyphae and no resistance offered by the broth these attempts were unsuccessful. Because of this 1% PYG with low melting point agar was used to carry out mass flow trials.

Chip inoculation with agar

Due to the lack of success with the channels filled with broth, to offer more purchase 1% PYG media with low melting point agar was used to fill the channels. The PYG media contained [in gL^{-1}; glucose 3 (Sigma Aldrich Chemicals Pvt. Ltd., India); bacteriological peptone 1.25 (Oxoid Ltd., England); yeast extract 1.25 (Oxoid Ltd., England); and bacteriological agar 10 (Invitrogen^{TM}, USA)]. After autoclaving, sterile glass vials were filled with 5 mL of this media and stored at 4^0C. The chips were kept in a dry agar oven at 50^0C for 2 hrs prior to addition of the agar. By keeping the chips warm, this was intended to help the even flow of the agar media through the channels. The media filled vials were kept in a water bath heated to 65^0C. The vials were then opened in the sterile environment of the LAF hood and using a 20 µL micropipette the media was introduced into the chip. Flow of agar was observed under the microscope and once the channels had filled and then set, the solidified agar at the seeding area end was removed and an inoculation plug was inverted and placed into the chip. More media was added on top to maintain moisture content. Growth rates were measured once the hyphae entered the channel and attempts to microinject oil were carried out once the hyphae had exited the channel or at the plug end (Figure 2.7).

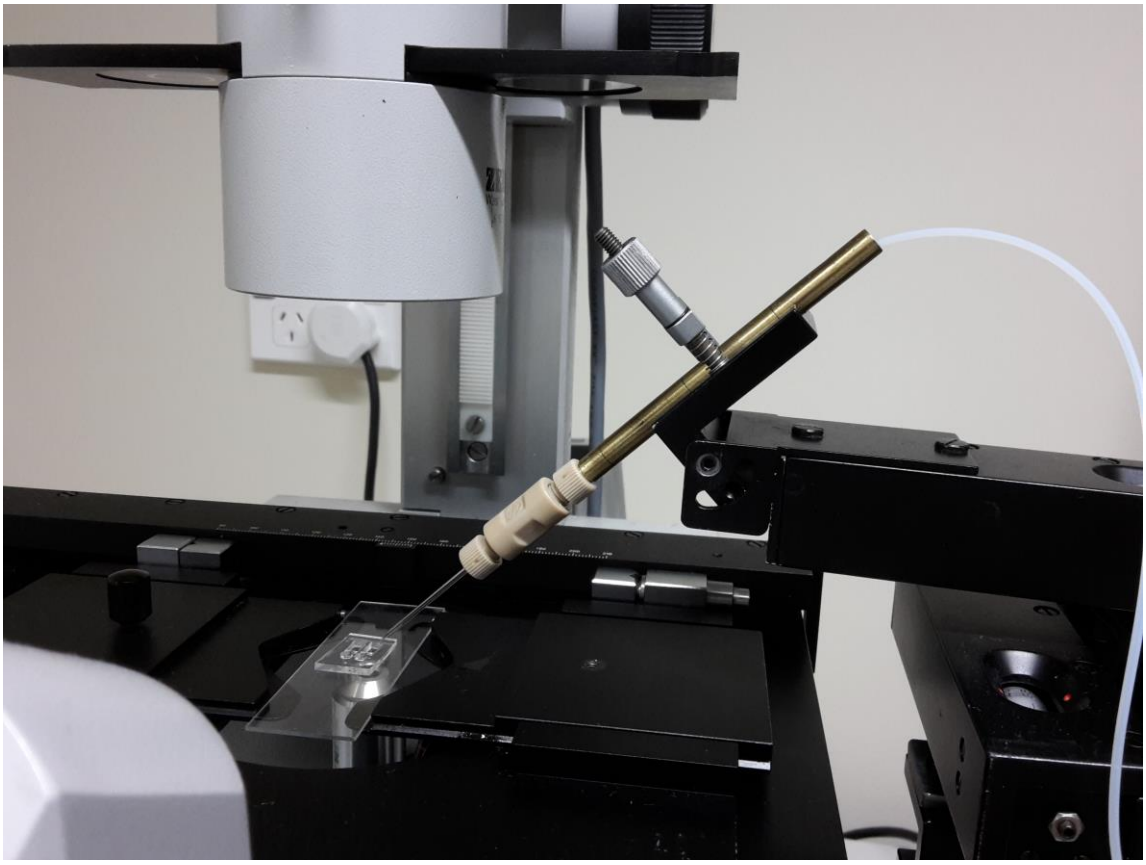

Figure 2.7: Set-up for microinjecting silicone oil into hyphae on a PDMS chip. The glass micropipette is held in the brass holder and filled with silicone oil. This is aligned with a single hypha, which grows along the micro-channel and exits out. Microinjection is carried out in this exit area.

2.9 Software and Statistics

The analysis of all data was carried out in ImageJ-win64.

Movement of oil droplet

Images were taken every 10 s on a USB 3.0, xiQ, Ximea camera. The rate of observed mass flow was calculated by measuring the movement of the droplet after the addition of hyperosmotic/ hypoosmotic solution. These images were compiled into a stack and using the region of interest (ROI) tool a label was placed at the edge of the droplet. Using the straight-line draw tool measurements were made by checking distance from the label to the edge of the moving droplet for each image. The scale was set by converting the scale of micrometer under the 10 X objective lens to pixels.

Growth rate measurements

The growth rates were measured in ImageJ-win64. The images were compiled into a stack and the distance was measured between the images after a set time using the straight-line draw tool.

Statistics

The mean values, standard deviations and standard mean errors were calculated using Microsoft Excel.

Chapter 3 Results

3.1 Micropipettes

Impaling the hyphae in an invasive condition i.e. growing through the media, involved pulling different micropipettes using a pipette puller as described in Chapter 2. To inject an oil droplet into a hypha, with minimum damage to the cell wall, several pipettes with varying tip sizes were tested. Pipettes (I.D. 1.17 mm) were prepared at different VUs these included 55, 56, 57 and 64 VU. The pipettes pulled at 55 and 56 VU were unsuitable for oil microinjection for the following reasons. At 55 VU the pipettes became clogged with biological material after they were inserted into a hypha presumably due to a wound response. This inhibited the flow of oil out of the pipette even though pressure was applied for several min and this further resulted in the leakage of oil once the pipette was pulled out of the cell. Pipettes pulled at 56 VU left a larger wound at the site of impalement on the hyphal wall, compared to those pulled at 57 and 64 VU. This resulted in the hypha failing to reseal itself after impalement, resulting in the silicone oil droplet leaking out of the cell. Hence, initial mass flow trials were carried out using the pipettes pulled at 57 VU. While these pipettes allowed the injection of oil and testing of mass flow, they often left a large wound on the cell wall at the site of impalement. The micropipettes pulled at 64 VU left very small wounds at the site of impalement but due to the narrowness of the tip more pressure was required to release oil in the cell. Due to their fine tip, plugs tended to form around them due to a wound response, which posed problems when trying to extract the pipette out of the cell. Hence, several trials were discarded as the pipette was left lodged within the cell.

The second set of borosilicate tubes used to produce micropipettes had a smaller inner diameter (I.D.0.86 mm). When these pipettes were pulled at 64 VU they gave the most suitable micropipettes for oil injection. They impaled the hyphal cells with ease and with minimum damage, allowing for smaller droplets to be injected within the cell after exertion of pressure.

The size of silicone oil droplets injected into the cell ranged from 14 µm to 48 µm in diameter. Droplets that were smaller than 20 µm in diameter did not move during either hyper- or hypoosmotic shock. The reason for this is not known but could be due to the wound response causing vesicular material to surround and restrict movement of the drop.

3.2 Impaling of hyphae

The process of impalement of hyphae growing on a petri-dish required maneuvering of the micropipettes through agar to align them with a single hypha. The presence of agar added purchase for the process of impalement and hence invasive hyphae were easier to impale than non-invasive hyphae. The impaling of the hypha was carried out approximately 300 µm to 1.5 mm back from the tip of the growing hypha. In several cases when the oil was injected into the cell, there was pulsing of the oil for several seconds or alternately the entire hypha filled up with oil. In these cases, the trials were discarded. The hyphal width at the site of impalement ranged from 20 to 51 µm. The process of impalement of a hypha in petri-dish is shown in Figure 3.1.

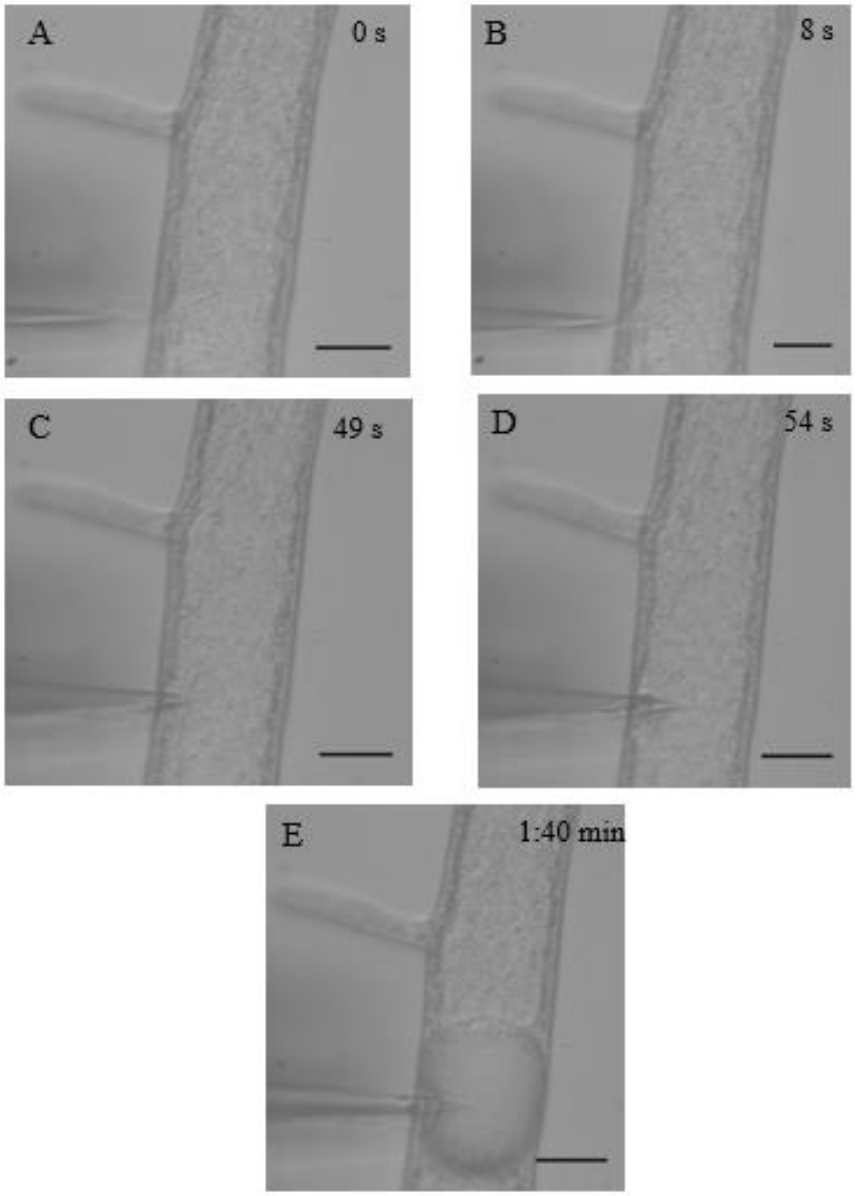

Figure 3.1**:** Microinjection of a single invasive hypha growing on a petri-dish using micropipette pulled at 64 VU under 10 X objective lens A) Aligning the micropipette with a single hypha on the plate B) Micropipette at the cell wall of the hypha C) and D) Impaling the cell and exertion of pressure for release of oil E) Oil droplet formation within the cell. Scale bar 30 µm.

3.3 Change of pressure gradients

Hypoosmotic treatment

The osmolality of the PYG broth was measured as described in Chapter 2. The average osmolality was 23.3 ± 1.2 mOsmol. Kg^{-1} (mean ± SEM) in the absence of agar. A hypoosmotic treatment was delivered to the hypha by addition of 20 µL of distilled water, approximately one cm away from the site of impalement. To estimate the osmotic shock received by hyphae the change in osmotic potential was calculated by substituting the osmometer readings into the Van't Hoff equation

The Van't Hoff equation $\triangle \pi = -\triangle cRT$ where $\Delta\pi$ is the change in osmotic potential, Δc is the concentration of solutes, R is the universal gas constant (0.0083 (MPa L). mol K) and T is absolute temperature (293 K).

The change in osmotic potential was calculated to be ∼-0.056 MPa as the distilled water was added, which is designated as time 0. For these calculations the osmolality of distilled water was 0 mOsmol. Kg^{-1} and the volume was 20 µL and osmolality of PYG broth was 69.9 mOsmol. Kg^{-1} and the volume was 3 mL.

Hyperosmotic treatment

To elicit a hyperosmotic shock, 20 µL of sorbitol solution was added approximately one cm from the site of impalement. Three different concentrations of sorbitol were tested, 0.25 M, 0.5 M and 1 M which have osmolality values as described in Table 2.1 in Chapter 2. After initial experiments all subsequent hyperosmotic trials were carried out using the 0.5 M sorbitol solution. The osmolality of this solution was 491± 2.5 mOsmol. Kg^{-1} (mean ± SEM) and hence the osmotic shock delivered to these organisms was ∼-0.064 MPa at time 0 as calculated using the Van't Hoff equation.

3.4 Mass flow trials

Hypoosmotic trials

A total of 20 trials were conducted by adding distilled water subapical to the impalement site (or towards the mycelium end). The hypha chosen for impalement were all invasive and grew in

different directions on the culture plate. According to the principle of mass flow the movement of the oil droplet should be in the anterograde direction. Seventeen out of 20 i.e. 85% of the droplets moved in the predicted direction, while 2 out of the 20 i.e. 10% did not move (both of these oil droplets had a diameter that was less than 20 µm). It took 3 ± 2 s (mean ± SEM) for the droplet to start moving during these trials and they moved for an average time of 1:50 ± 0:8 min (mean ± SEM). During one trial (i.e. 5% of tests), the droplet moved in the opposite direction to that which was predicted. The droplet started to move 15 s after the osmotic shock and it continued to move for 2:5 min. The movement of oil droplets after hypoosmotic treatment is represented in Table 3.1. The reason for this is unknown, but it should be noted that the petri-dish is not the most streamlined and addition of either hyper- or hypoosmotic solution is not in a contained area. A representation of droplet movement in anterograde direction is as shown in Figure 3.2.

In cases where a branch was present near the injected oil droplet, movement of the droplet along with cytoplasm containing more contrasted organelles was observed within the branch and is shown in Figure 3.3. Without a change in the pressure gradient, the droplet failed to enter the branch, which might suggest that mass flow was occurring within the branch.

To test if mass flow occurred in the opposite direction 20 µL of distilled water was added at the tip end of the impaled hypha. During most of the trials, the impalement site was very close to the tip and with the addition of 20 µL of the hypoosmotic solution, the solution would flow over the oil droplet in the hypha resulting in a loss of optical clarity. Hence, for the subsequent trials the water was added in 5 µL aliquots. In these trials the droplet did not move till all the 20 µL had been added. A total of 6 trials were conducted to test mass flow towards the mycelium end. In 5 out of the 6 trials i.e. ~83% the oil moved in the predicted direction towards the mycelium end. In the other trials i.e. ~16 % the oil did not move. In this trial the droplet diameter was less than 20 µm. Oil movement in the retrograde direction after hypoosmotic treatment is shown in Figure 3.4.

Table 3.1: The direction of oil movement was driven by a pressure gradient in majority of hyphae upon hypoosmotic treatment apically and sub-apically

Oil movement	Side of hypha where osmotic shock was delivered	
	Subapically	Apically
Predicted direction of oil movement if mass flow is occurring	Anterograde	Retrograde
Number of hyphae showing anterograde oil movement	17 of 20 (85%)	0 of 6
Number of hyphae showing retrograde oil movement	2 of 20 (10%)	5 of 6 (83%)
Number of hyphae showing no oil movement	1 of 20 (5%)	1 of 6 (16%)

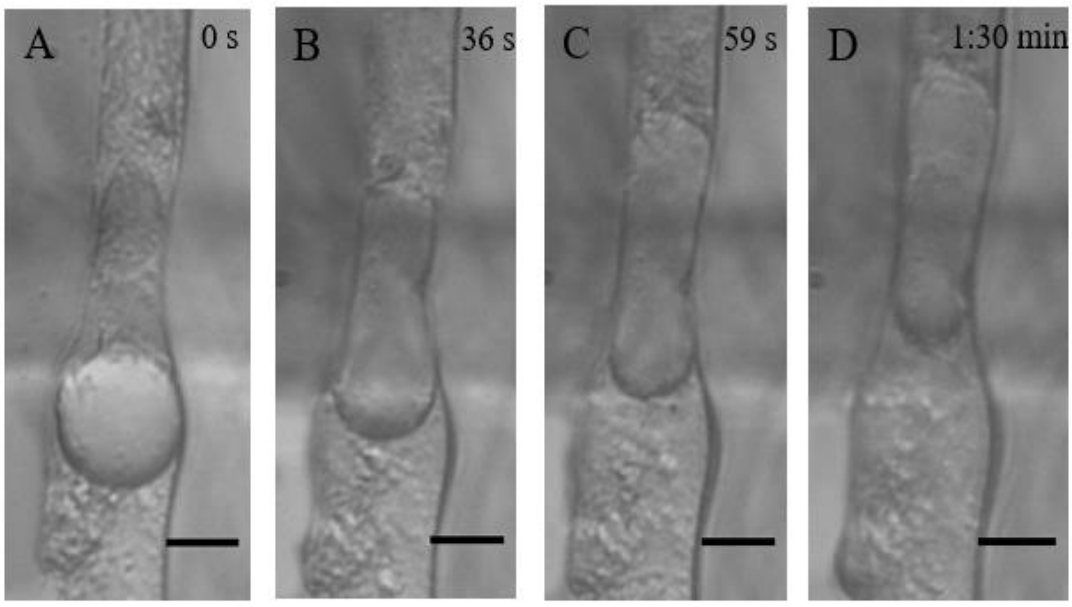

Figure 3.2: Anterograde movement of oil droplet within hypha after hypoosmotic treatment subapically A) Oil droplet injected within hypha B) Movement of oil in anterograde direction C) & D) Anterograde movement through the narrower section of the hypha. Scale bar 20 μm

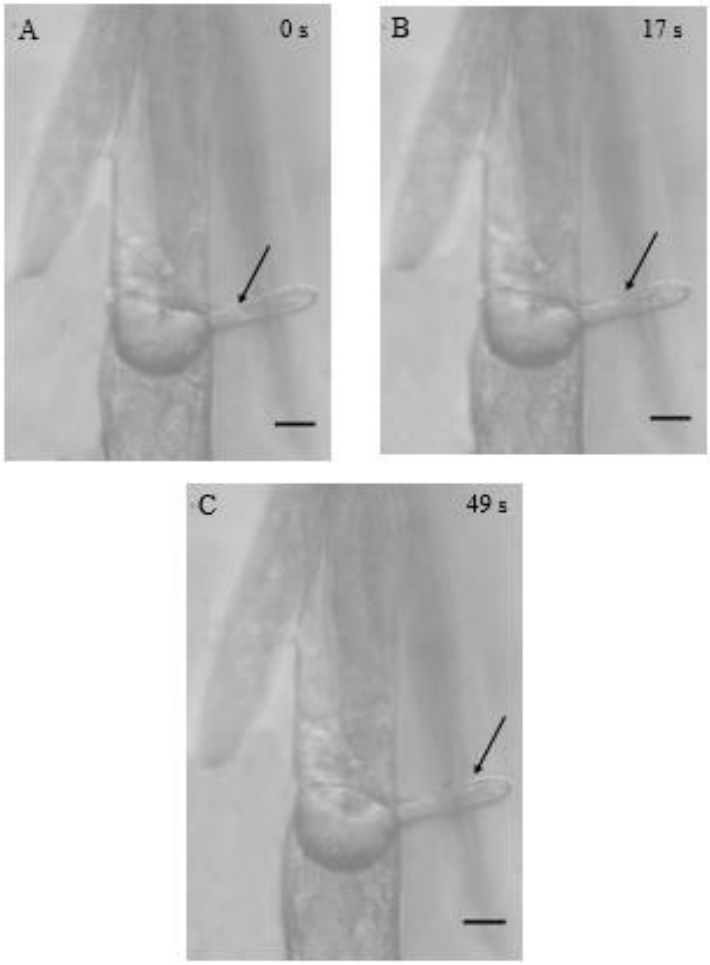

Figure 3.3: Movement of oil droplet along with cytoplasm containing more contrasted organelles into a side branch upon hypoosmotic treatment. A) Arrow points to the movement of cytoplasm containing more contrasted organelles entering the branch B) Side branch half fills with the above mentioned material C) Side branch filled till the tip with oil and cytoplasm containing more contrasted organelles. Scale bar 20 μm.

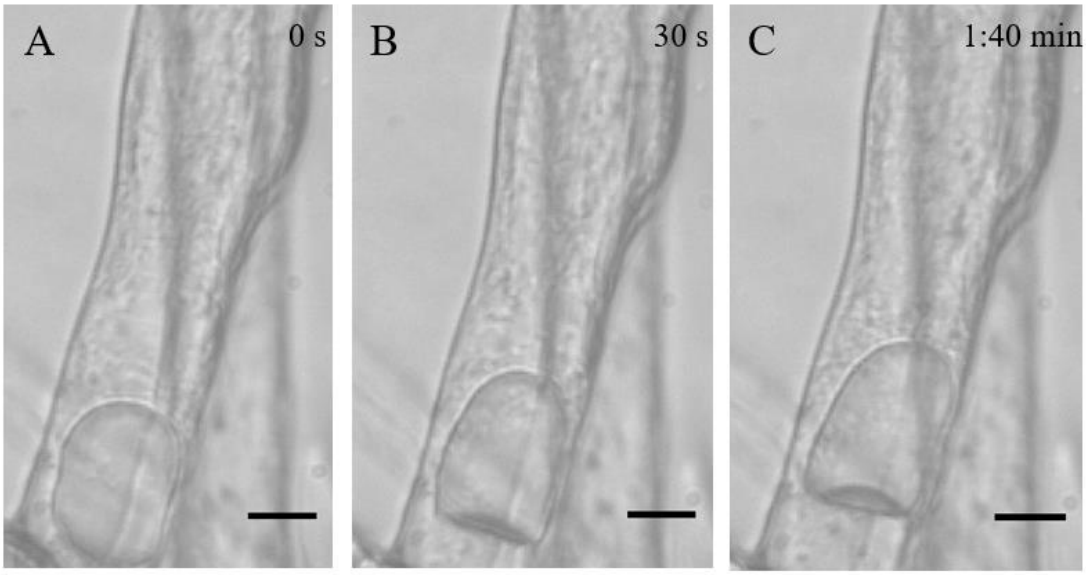

Figure 3.4: Movement of an oil droplet in retrograde direction after an apical hypoosmotic treatment (bottom end of the image). A) The formation of an oil droplet within the hypha B) & C) Movement of the droplet in retrograde direction towards the subapical region within hypha after hypoosmotic treatment. Scale bar 20 μm.

Hyperosmotic trials

A total of 12 hyperosmotic trials were conducted. These included the addition of 20 µL of a 0.5 M sorbitol solution subapical to the impalement site. According to the principle of mass flow this would involve the droplet moving in the retrograde direction. In 7 out of 12 trials i.e. ~58% of trials the droplet moved in the predicted direction in a retrograde direction, while in the case of 5 out of 12 i.e. ~41% cases the droplet moved in an anterograde direction, toward the tip end (Table 3.2). The droplets moved for an average time 2:2 ± 0:2 min (mean ± SEM) after the addition of the hyperosmotic solution. The reason for this is not known. The movement of a droplet after the hypha has been exposed to a hyperosmotic treatment is shown in Figure 3.5.

A single trial was carried out in, which sorbitol was added towards the tip end in order to investigate if mass flow occurred in the opposite direction. The droplet moved in the predicted direction, in the anterograde direction.

As was for the hypoosmotic trials, oil was observed to move into branches close to the impalement site when the hyperosmotic treatment was imposed as depicted in Figure 3.6

Table 3.2: The direction of oil movement was driven by a pressure gradient in majority of hyphae upon hyperosmotic treatment sub-apically

Oil movement	Side of hypha where osmotic shock was delivered Subapically
Predicted direction of oil movement if mass flow is occurring	Retrograde
Number of hyphae showing retrograde oil movement	7 of 12 (58%)
Number of hyphae showing anterograde oil movement	5 of 12 (41%)
Number of hyphae showing no oil movement	0 of 12

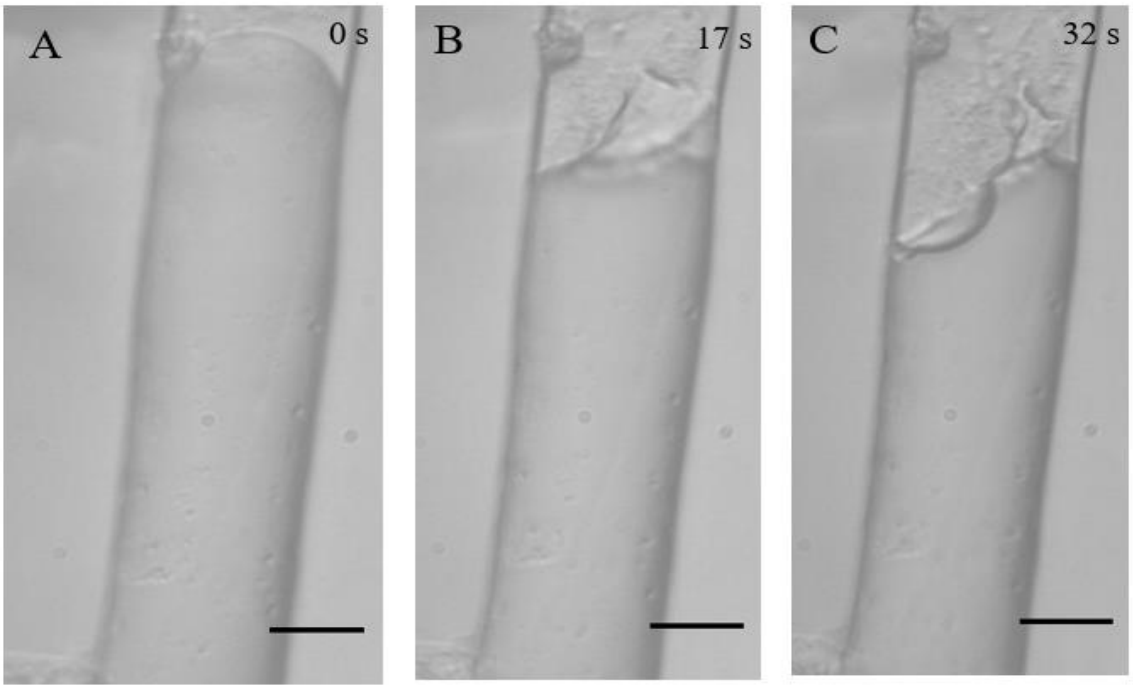

Figure 3.5: Movement of oil in a retrograde direction within a single hypha after hyperosmotic treatment towards the subapical region. A) The oil droplet is injected into the cell B) & C) The oil droplet moves in the retrograde direction after the subapical hyperosmotic treatment. Scale Bar 30 µm.

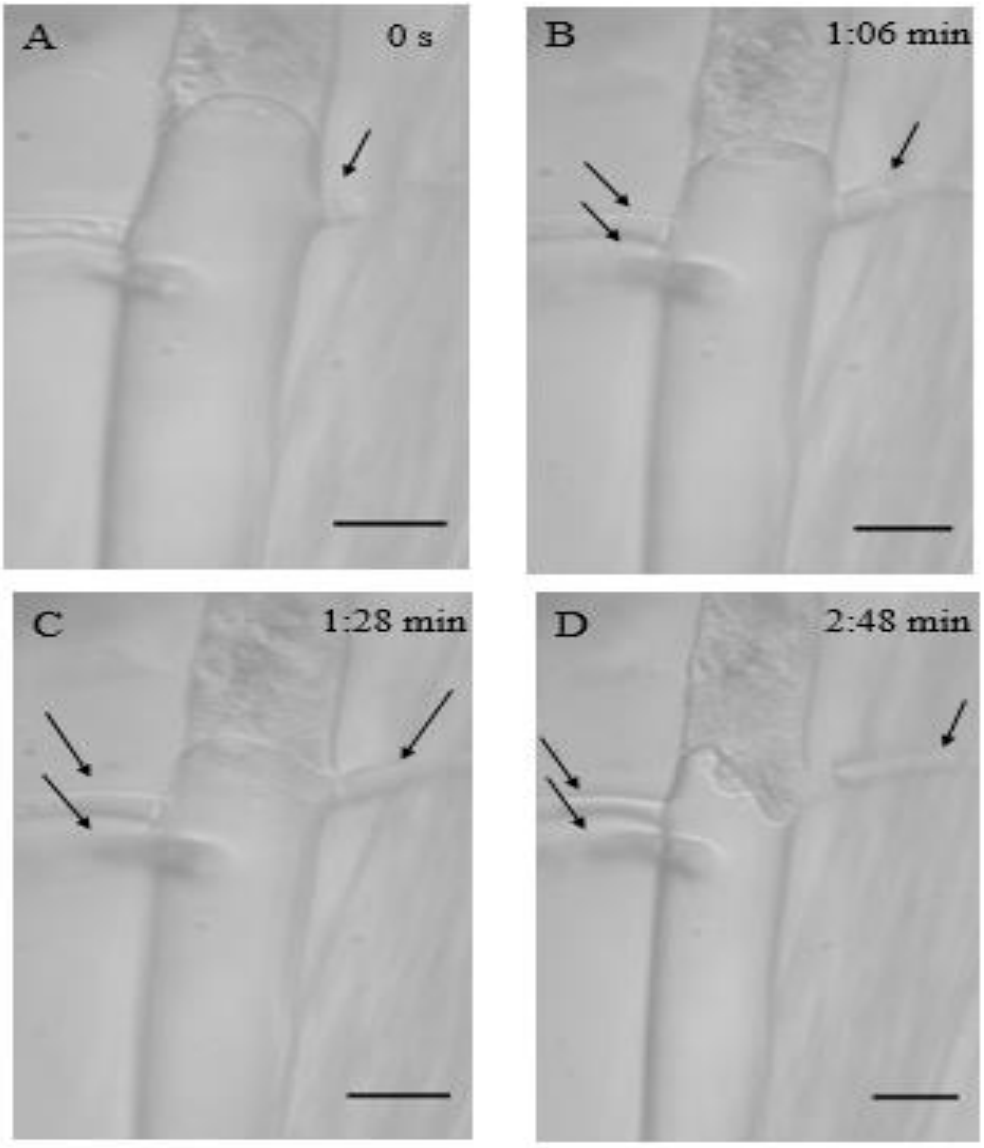

Figure 3.6: Movement of oil in a retrograde direction within a single hypha after hyperosmotic treatment towards the subapical region. A) Arrow shows the initial entry of oil into one branch B), C) & D) Oil movement in the three side branches as represented by the arrows. Scale bar 30 µm.

Oil movement in the absence of any pressure gradient

A total of 6 trials were conducted, in which oil was injected but there was no addition of a hypo- or hyperosmotic solution. In all these trials, there was compression of the oil droplet at the subapical end, but no forward movement was noticed. The compression could be due to cytoplasmic contraction of a wound response.

3.3 Mass flow rates

Hypoosmotic treatment

The measured rate of movement of oil in an anterograde direction after subapical hypoosmotic treatment was 0.3 ± 0.05 µm s^{-1}(n=17) (mean ± SEM). One drop moved in the retrograde direction (i.e. opposite to predicted direction). It had the rate of 6.6 µm s^{-1} (n=1). Movement of oil droplet in retrograde direction after apical hypoosmotic treatment was 0.4 ± 0.2 µm s^{-1}(n=6) (mean ± SEM). If we consider the hyphae as a continuum of pipes and the flow within them to be laminar, then we can calculate a theoretical rate of mass flow using the Hagen-Poiseuille equation

$$\nu = \frac{\pi R^4 \mid \triangle P \mid}{8\eta L}$$

where R= radius of hyphae, ∆P = pressure gradient, η = viscosity and L = hyphal length. The viscosity in this case is taken to be η = 1X 10^{-3}, which was reported for the cytoplasm of fibroblasts (Fushimi & Verkman, 1991). This same value of viscosity was used to calculate the theoretical value of mass flow in *N. crassa* hyphae and in mycelia of *A. bisexualis* (Lew, 2005; Muralidhar et al., 2016). Taking the values of observed hyphal length and width from the Table.3.3 and substituting in the Hagen-Poiseuille equation a theoretical rate of oil movement is shown in Table.3.4.

Table 3.3: Mean hyphal lengths and widths at the site of impalement during hypoosmotic trials

	Anterograde	Retrograde
Mean hyphal length (SEM)	912.6 ± 169 µm	1426.6 ± 274.7 µm
Mean hyphal width (SEM)	17.71 ± 2.3 µm	20.8 ± 0.9 µm

Table 3.4: Mean rates of oil droplet movement and the theoretical rates calculated using Hagen-Poiseuille equation for hypoosmotic trials

Oil movement	Side of hypha where osmotic shock was delivered	
	Subapically	Apically
Predicted direction of oil movement if mass flow is occurring	Anterograde	Retrograde
Mean speed of anterograde oil movement	3×10^{-7} m s^{-1}	6.6×10^{-6} m s^{-1}
Theoretical rate	0.23×10^{-8} m s^{-1}	———
Mean speed of retrograde oil movement	_____	4×10^{-7} m s^{-1}
Theoretical rate	_____	0.29×10^{-8} m s^{-1}

Hyperosmotic treatment

With hyphae that were exposed to a hyperosmotic shock, the average rate of mass flow was observed to be 0.14 ± 0.05 µm s^{-1} (n = 7). Taking the values of observed hyphal length and width from Table 3.5 and substituting these in the Hagen-Poiseuille equation a theoretical value of mass flow was calculated to be 0.33×10^{-8} m s^{-1} (Table 3.6).

Table 3.5: Mean hyphal lengths and widths at the site of impalement during hyperosmotic trials

	Retrograde
Mean hyphal length (SEM)	1056.8 ± 260.7 µm
Mean hyphal width (SEM)	19.3 ± 0.9 µm

Table 3.6: Mean rates of oil droplet movement and the theoretical rates calculated using Hagen - Poiseuille equation for hyperosmotic trials

Oil movement	Side of hypha where osmotic shock was delivered Subapically
Predicted direction of oil movement if mass flow is occurring	Retrograde
Mean speed of retrograde oil movement	1.4×10^{-7} m s^{-1}
Theoretical rate	0.33×10^{-8} m s^{-1}

3.4 Change in hyphal tip shape after mass flow

The shape of the hyphal tip was observed to change after both hypo- and hyperosmotic treatment Figure 3.7. The tip became less tapered and more rounded possibly due to a cessation of polarized growth.

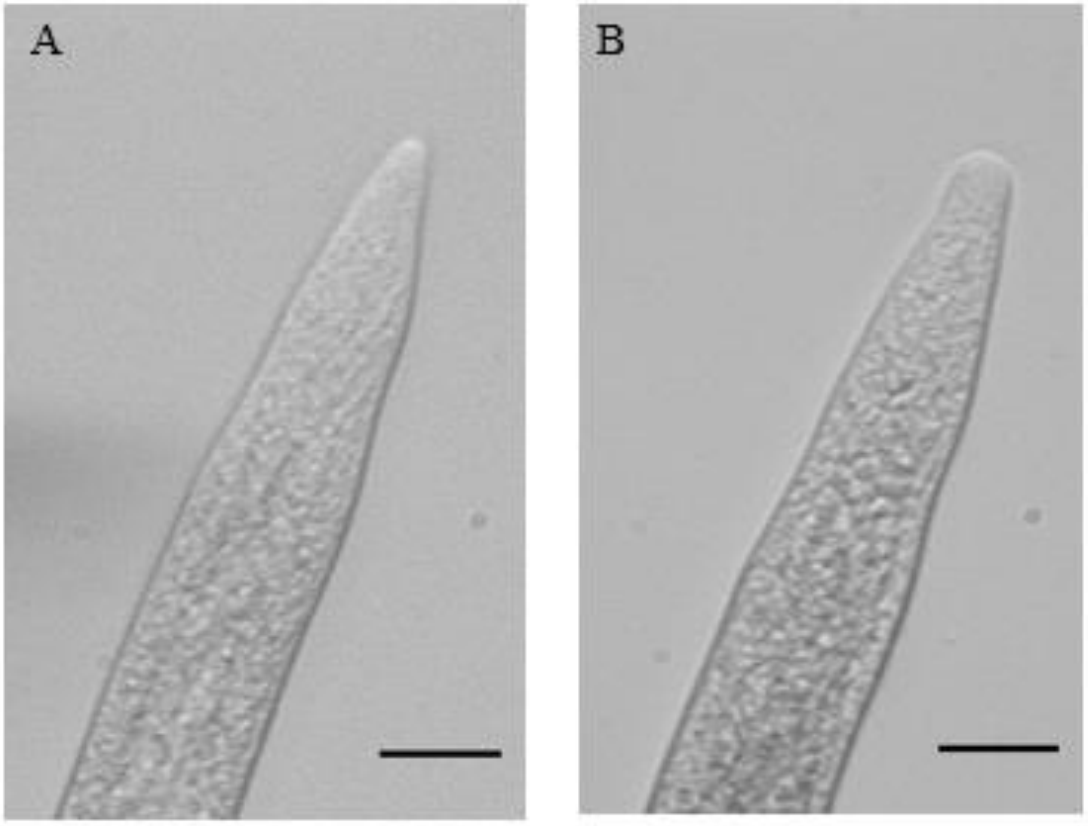

Figure 3.7: Change in hyphal tip shape after hypoosmotic treatment A) The hyphal tip before the treatment with hypoosmotic solution B) After treatment the tip appeared less tapered and more rounded. Scale bar 30 µm.

Speed of oil droplet vs width of the hypha

During one of the hypoosmotic trials the oil droplet was microinjected in a wider part of the hypha as shown in Figure 3.2. To check if the width of the hypha affected the rate of movement of the oil droplet, the rate of movement over a 10 s period was compared to the hyphal width. The observed movement of oil droplet was at a rate of 14.6 µm/10 s was observed when hyphal width was the narrowest of 16.7 µm diameter.

3.5 PDMS chips, growth rates and mass flow

Chip design 1

The design of the first set of chips was as mentioned in Chapter 2. These chips were discontinued after a few trials due to the dislodging of the plug from the seeding area and the formation of air bubbles within the chip during an experiment. The dislodging may have been caused by the increased pressure exerted by the introduction of excess broth through the ports during feeding. The growth rate of *A. bisexualis* in the channels of these chips is noted in Table 3.7.

Chip design 2

The design of the second set of chips is as described in Chapter 2. With these chips, it was noted that the broth did not fully fill the channels. The absence of broth caused the hyphae to grow poorly on these chips and it took the hyphae several days to enter the channels and a day to grow along the channels. Because of this it was difficult to accurately measure the growth rates of hyphae on these chips. These chips were discontinued after several trials.

Chip Design 3

The design of the third set of chips is as described in Chapter 2. With these chips an increase in degassing time was attempted in order to improve the flow of broth into them but this did not change the flow rate of the broth down the channels. However, the hyphae grew on these chips but at a slower rate (Table 3.7).

Chip design 4

The design of the fourth chip is as mentioned in Chapter 2 and since they still had problems with the flow of broth into the channels of these chips they were discontinued. No growth rates were taken on these chips as hyphae struggled to grow on them.

Chip design 5

The design of the fifth chip is as described in Chapter 2. Growth of hyphae was observed on these chips in both non-invasive (PYG broth) and invasive (1% agar) conditions (Figures 3.8 & 3.9). Growth rates are detailed in Table 3.7.

Table 3.7: Growth rates of the hyphae along PDMS channels on different chip designs

Chip Design	Growth rates per minute
Design 1	4.3 μm min^{-1} ± 0.3 (n=5)
Design 3	3.6 μm min^{-1} ± 1.3 (n=8)
Design 5	5.2 μm min^{-1} ± 0.3 (n=12)
Design 5 (invasive condition)	3.9 μm min^{-1} ± 0.06 (n=3)

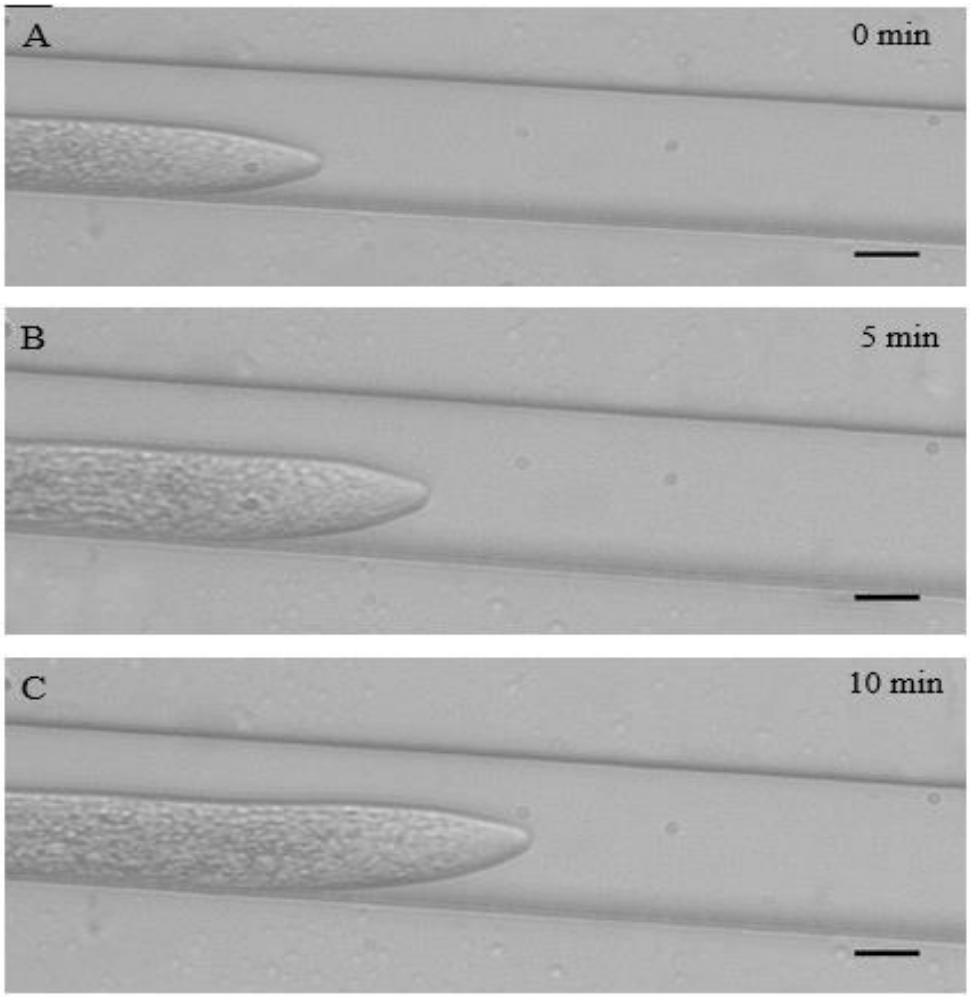

Figure 3.8: Growth of a single hypha along a channel on a PDMS chip. The channel was 35 μm in width and 3 mm in length. The hypha is growing non-invasively through PYG broth A) 0 s B) 5 min & C) 10 min. Scale bar 20 μm.

To test for mass flow in hyphae growing on chips, hyphae were impaled in the exit area of the channel as is shown in Figure 3.8. Attempts at impalement were initially carried out on hyphae that were growing in PYG broth. Due to the lack of purchase owing to the presence of only broth within the channels of the chip, impalement was unsuccessful.

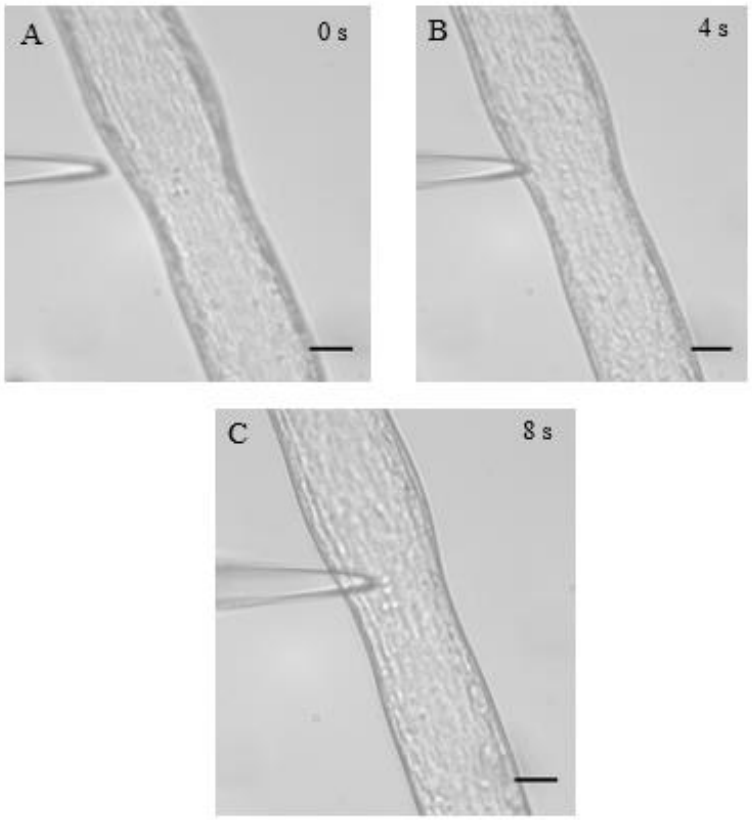

Figure 3.9: The process of impaling single hypha growing along a channel on a PDMS chip. The micropipette deflected the hypha in the broth but failed to impale it due to a lack of purchase A) Alignment of the micropipette with a single hypha B) & C) Attempt to microinject and the deflection of the hypha. Scale bar 20 µm.

Invasively growing hyphae on a chip

To overcome the difficulty of impaling non-invasive hyphae, invasive conditions were invoked by pouring 1% agar on the chip. Hyphae grew at the described rates in Table 3.7 and as shown Figure 3.8. Thus, attempts were made to impale the hyphae but unfortunately 1% agar did not provide sufficient purchase to enable successful impalement.

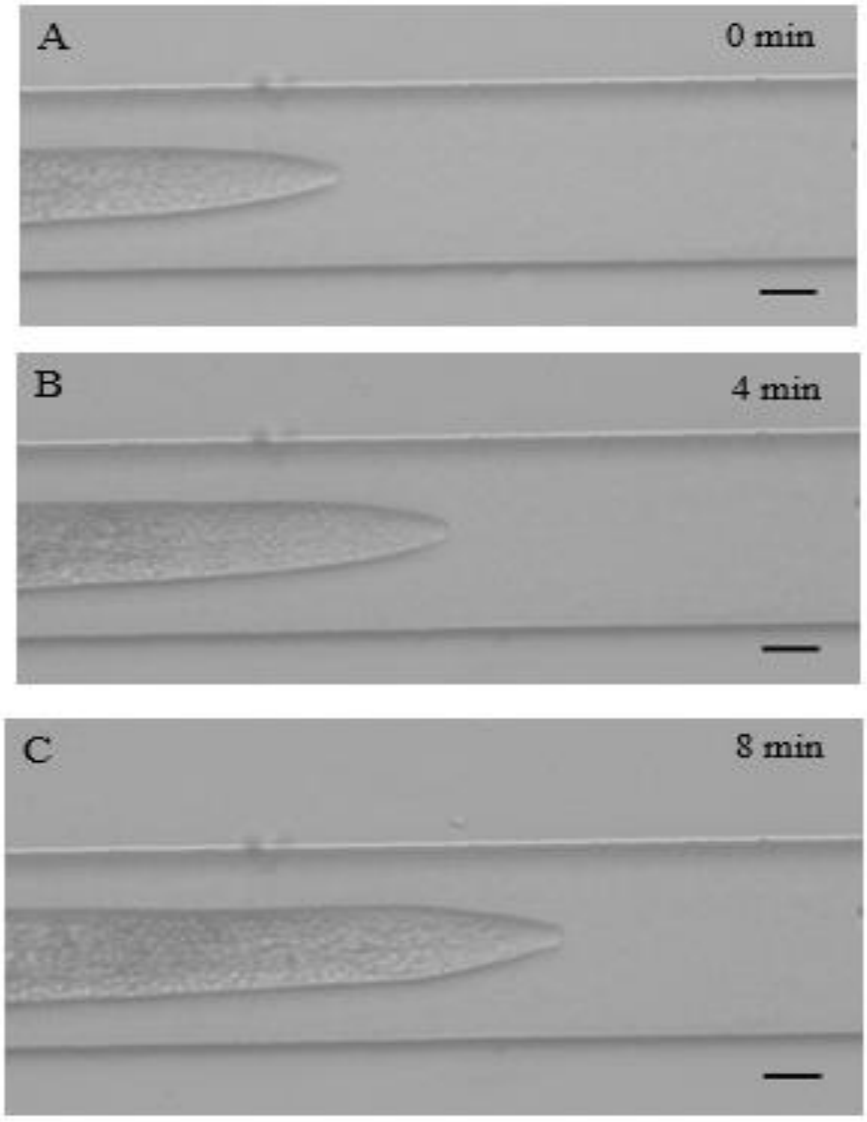

Figure 3.10: Growth of a single hypha along a channel on a PDMS chip. The channel was 35 µm in width and 3 mm in length. The hypha is growing invasively through 1% PYG agar A) 0 s B) 4 min & C) 8 min. Scale bar 20 µm.

Chapter 4. Discussion

Mass flow is a term that is used to describe the bulk movement of material down a pressure and/or temperature gradient. It has historically been used to describe the movement of material in plants but as described further below, mass flow and the generation of pressure gradients that drive the process are of increasing interest in fungi and oomycetes as the process could play a role in the growth of these microorganisms (Angeles et al., 2004).

4.1 Mass flow in plant systems

The transfer of sap, water, gases and minerals within plant systems have been suggested to be driven by mass flow (Grosse, Armstrong, & Armstrong, 1996). In 1873, Feddersen reported the continuous flow of gas within an aquatic plant system across an artificial porous partition. This movement of gas was suggested to be due to the establishment of a temperature gradient and the gas movement occurred from the cooler to the warmer side (Grosse et al., 1996). Evidence from the aquatic macrophyte *Nelumbo nucifera* shows the transport of gases is independent of its physiological status (including photosynthesis) and dependent on a physical effect. Thus, the air space system within these plants might be considered as a continuous system extending from the rhizome to the leaf and continues onto another leaf. In wetland plants such as the Yellow Water-lily, have a similar mechanism of gas transfer to that of aquatic plants. When these plants were injected with ethane it resulted in the bulk flow of the gas against raised pressure within the aerenchyma (Grosse et al., 1996).

Other than the gas transfer in plants, mass flow has been associated with the movement of sap/water in higher plants. Larger trees, which scale several meters tall require transport of water daily to the crown area feeding the growing leaves and branches. Two primary systems, which perform this function include the phloem and xylem. Exudates of phloem have osmotic pressures of 1.2 to 1.8 MPa, and a pH of 8.0 to 8.5, which is concentrated with amino acids, reducing sugars such as sucrose and electrolytes. These are transported from the leaves to the various plant tissue. The xylem transports nutrients form the soil to the leaves. Hence, they act as transporting tubes from the source (roots in soil or leaves) to the sinks (higher branches and other plant tissue).

However, in man-made pump systems, water flow is observed only for several meters above the ground even in the absence of air bubbles within the system (Ziegler, 1975). For water/sap to scale 100 m heights in larger trees, the xylem and phloem are thought to work on the principle of mass flow. Cohesion theory, which is proposed for transport via xylem suggests that a pressure gradient is established due to evaporation on the surface of leaves resulting in increased surface tensions. The xylem cells transfer this tension allowing for transport of nutrients along with water to peripheral tissue (Dixon & Joly, 1894).

Transport in phloem is explained through the Münch hypothesis (Munch 1930). Here pressure gradient is established by the loading of osmotically active solutes such as sucrose at the leaves (source), and its removal and transfer from the sap (sink) to the tissues of the plant. (Ziegler, 1975). Contrary to this theory, the concentrations of potassium within the sieve tubes have been suggested to enable turgor driven translocation. Potassium concentrations have been related to maintaining of turgor within plants as they act as osmoticum (Lang, 1983).

Evidence suggests that water movement through a plant occurs as a result of a temperature gradient, which drives mass flow. This can be seen in the stems of herbaceous plants for example (J V Baker & Bavel, 1987). Direct measurement techniques have been employed to study the effects of temperature on the direction of water flow within the xylem. These techniques include the heat pulse technique for measuring the flow velocity in the xylem and the heat balance method for studies of stem flow. This latter technique has been modified with a new gauge design that enables measurement of water flow without injury or penetration of the cell (J V Baker & Bavel, 1987). However, NMR technology being used for study of translocation within plants has proved most effective as they are non-invasive and do not damage the host tissue (Windt et al., 2006).

4.2 Role of mass flow in fungi and oomycetes

Findings from studies of the mycelia of *A. bisexualis* and hyphae of *N. crassa*, show the movement of organelles to be independent of mass flow and likely driven by active transport with the help of motor proteins (Lew, 2005; Muralidhar et al., 2016). These typically move at rates of between 1.4 to 2.0 μm s^{-1}(Steinberg & Schliwa, 1993).

The passive movement of the nuclei due to cytoplasmic flow has also been reported in the hyphae of several fungi by live cell imaging. In these studies, data suggested that the nuclei at the apex would move as the hypha grew, maintaining an approximately constant distance from the tip (Heath, 1982; Herr & Heath, 1982). In *N. crassa* hyphae nuclei positioning is mainly suggested to be the result of cytoplasmic flow, however the role of motor proteins such as dynein has not been ruled out (Ramos-García et al., 2009). In *N. crassa* mutants, nuclear movement due to cytoplasmic flow is not prominent in germlings and does not occur until hyphal growth is established. The disruption of the cytoskeleton with drugs such as benomyl did not stop nuclear movement towards the tip, but the average rate of nuclei movement did decrease suggesting that cytoplasmic flow may play a role in this process (Ramos-García et al., 2009).

Other than nuclei, the movement of vacuoles and mitochondria have also been reported within *N. crassa,* using green fluorescent protein tags and fluorescent markers, which is suggested to be influenced by the mass flow of cytoplasm (Abadeh & Lew, 2013). The flow is thought to be the result of establishment of an intrahyphal pressure gradient, which was induced by external addition of osmotic solutions. Results of the velocity of organelle movement did not match those obtained by the Hagen-Poiseuille equation but instead fit models of partial plug flow, the reason for this was suggested to be the high concentration of organelles within the flowing cytosol (Abadeh & Lew, 2013).

4.3 Turgor Regulation and mass flow in fungi

The presence of an internal hydrostatic pressure or turgor within organisms, which possess cell walls, such as plants, fungi and oomycetes, is thought to play a key role in tip growth. This provides the driving force for growth, and arises due to the build-up of solutes within the cell leading to a difference in solute concentrations inside and outside the cell. Turgor causes the plasma membrane to push against the cell wall allowing cell expansion to occur at the plastic tip. In fungi and oomycetes differences in this pressure, along the long tubular hyphae may also contribute to growth in facilitating a pressure gradient that drives the movement of cytoplasm through the process of mass flow. If mass flow in hyphae is important for growth then it might be expected that hyphae should be able to control or regulate turgor (Lew, 2011; Lew et al., 2004; Money & Harold, 1992).

Turgor regulation in hyphal organisms has been studied when they are exposed to an osmotic shock. Direct measurements of turgor in the fungus *N. crassa* suggest that when it is challenged with a hyperosmotic shock of 0.6 MPa it can regulate its turgor and recover from the shock (Lew et al., 2004). Recovery was found to be correlated with changes in membrane transport processes in that there was a hyperpolarization of the membrane potential and a decrease in transmembrane ion conductance. These changes were proposed to increase the driving force for H^+- coupled anion uptake and electrophoretic K^+ uptake, movements that would counter the hyperosmotic treatment by increasing the osmolarity of the hyphae and facilitating turgor recovery (Lew et al., 2004). Additional synthesis of osmotically active solutes may also have been occurring. Similar mechanisms have been proposed for turgor regulation in the higher plant *Arabidopsis thaliana* exposed to a hyperosmotic shock (Lew, 1994; Lew et al., 2004; Shabala & Lew, 2002).

In *Morchella esclentum* translocation during the development of the sclerotia is suggested to be the role of turgor driven mass flow (Amir et al 1995). Previously, translocation in this organism was studied using an indirect method by noting the rate of movement of radiolabeled material from the mycelium to the sclerotia. Experimental set-up included a split petri-dish composed of different media on either side, with different water potentials. i.e. defined media on one side and glucose supplemented Nobel agar on the other. Rate of movement of [^{14}C] 3-O-methyl glucose and [^{14}C] D-glucose suggested that translocation might occur within the mycelium and sclerotia based on the biomass accumulation (Amir et al. 1994). The spilt petri-dish set-up could represent the environment where these organisms are exposed to different osmotic challenges.

The same experimental set-up was used to directly measure turgor pressure in the mycelium and sclerotia using a pressure probe. However, due to the small size of sclerotial tissue an indirect method of thermocouple psychometry was used for turgor measurement. Inoculation was carried out on the defined media side where the mycelium grew, while the sclerotia grew on the glucose supplemented Nobel agar side. To attract translocation of nutrients from the mycelium side, a low pressure has to be maintained on the sclerotial side. However, the sclerotial tissue needs pressure for cell expansion. Thus, the primary hyphae act as a low-pressure area as suggested by turgor readings of 0.7 MPa when compared to the turgor pressure measured indirectly in the sclerotial tissue of 1.2 MPa (Amir et. al. 1995). The pressure gradient created between the

sclerotia and mycelium measured a maximum pressure of 0.53 MPa. Thus, the hyphae at the edges on the mycelium side and the sclerotial tissue both acted as sinks, while the mycelium absorbed nutrients from the media (source) and translocated it to the growing edge on either side. Data suggested a change in direction of translocation at three different times, first translocation was noticed toward the hyphae at the mycelium end during extension and when this mycelium reached the edge of the plate, reverse translocation was observed towards the sclerotial side. Upon sclerotial maturation reverse translocation occurred at the mycelium end again. The pressure gradient was measured to be 0.53 MPa, which was concluded to be sufficient to allow for translocation of nutrients and other cellular components to the sclerotia and peripheral cells of the hyphal colony (Amir et al., 1992, 1994).

In addition, the microinjection of silicone oil droplets in hyphae of *N. crassa* using a pressure probe apparatus has supported the existence of a pressure gradient and mass flow. Since *N. crassa* provides a simpler system to those of Basidiomycetes such as *Armillaria mellea* and *Serpula lacrimans* where mass flow was studied using radioactive tags (Jennings, 1987), it was chosen to test mass flow within a single hypha, using a more direct method. The injection of silicone oil and tracking of the movement of oil droplets is thought to show mass flow as the oil is unlikely to move through the action of the cytoskeleton and molecular motors, since the oil droplets do not bind to either of these cellular components. The droplet would move upon the establishment of a pressure gradient created by the external addition of 1 M sucrose and basal salt solution (BS). Data showed that maximum number of droplets moved in the predicted direction depending on the region where the osmoticum was added. If septal pores were present the droplets 'blebbed' through them as they moved in the predicted direction. The direction of movement of the droplets was consistent with the movement of particles observed within the cytoplasm towards the hyphal tips. The highest cytoplasmic flow rate of 60 μm s^{-1} was observed. The rates of movement of oil droplets within *N.crassa* correlated to the rate of tip growth in these hyphae and so, in fungi it has been suggested that mass flow contributes in the process of tip growth (Lew, 2005). Mass flow was inhibited in experiments when the hyphae were exposed to 10 mM NaCN which would inhibit the proton pump (Lew, 2005). This was used to suggest that internal pressure gradients might be set-up due to the transport of ions via the proton pump and/or alternately the production of osmolytes.

4.4 Turgor regulation in oomycetes

The question of whether or not the oomycetes can turgor regulate is far from clear. As detailed in Chapter 1, a hyperosmotic shock treatment of 0.59 MPa with a 0.5 M sorbitol solution, which when administered to *A. bisexualis,* resulted in a decrease in turgor from which the hyphae were unable to recover. This led to the conclusion that, in contrast to fungi, oomycetes are unable to turgor regulate. However, this has come under question as two other Stramenopile species, *Vaucheria erythrospora* (dwelling in estuarine habitats) and *Vaucheria repens* (living in freshwater habitats), both yellow green algae, which share a recent common ancestor with *A. bisexualis,* have been shown to be able to regulate turgor after both hyperosmotic and hypoosmotic conditions. The magnitude of the shock from which the two species could recover differed and this was thought to be due to the fact that they occupy different habitats as *V. erythrospora* was able to turgor regulate after larger shocks. *V. erythrospora* is an estuarine species and is thus subject to constant osmotic changes due to the tidal cycle, whereas *V. repens* is a freshwater species and subject to a more homogeneous osmotic environment (Muralidhar et al., 2013). Direct measurement of turgor using a pressure probe showed that *V. erythrospora* was able to recover from hyperosmotic shocks of 0.5 MPa, whereas *V. repens* was only able to recover from shocks of 0.2 MPa. At osmotic shock that were tested above these values (0.8 MPa for *V. erythrospora* and 0.5 MPa for *V repens*) there was no turgor recovery. The ability to regulate turgor in these organisms is suggested to be a result of the action of several channels including mechanosensitive channels, nonselective cation channels and K^+ channels as observed by the inhibition of turgor regulation by the action of Gd^{3+} and TEA on these channels (Muralidhar et al., 2015).

The fact that these Stramenopile species could turgor regulate raised the question of whether the inability of *A. bisexualis* to turgor regulate in the earlier study was simply due to the fact that the shock imposed could be too large for it to recover from (Lew et al., 2004). Hence, lower concentrations of osmolytes might have yielded different results and this is clearly an area where more work could help clarify if oomycetes are indeed able to turgor regulate.

Ca^{2+} sensitive channels, which have previously been associated with turgor regulation in stromal guard cells of plants, is suggested to play a role in turgor regulation in oomycetes (Garrill, Lew, & Heath, 1992). Electrophysical studies on *S. ferax* have reported two K^+ channels in protoplast

of this oomycete which are activated by Ca^{2+} ions. Other than these channels, stretch activated channels were also observed in the PM of these organisms. The movement of ions through the K^+ channels is inwards and was suggested to enable turgor regulation, while stretch activated channels might play a role in tip growth by maintenance of turgor homeostasis. The solute influx calculated for these K^+ channels was 160 pA, a magnitude which was suggested to enable maintenance of turgor within the cell. The stretch activated Ca^{2+} channel might play a role in monitoring the turgor within the cell, acting as a sensor to register change in osmolytes across the PM (Garrill et al., 1992).

However, even if oomycetes are unable to turgor regulate and set up internal pressure gradients through membrane transport processes, the gradient could still arise due to differences in the concentrations of solutes in the environment along the length of a hypha. Although for this to occur and play a role in growth the gradient would have to be such as to enable bulk movement of the cytoplasm from a region of high pressure to the area of lower pressure within the hypha in turn transporting nutrients to the tip and applying pressure on the plastic tip allowing it to undergo cell expansion.

4.5 Mass flow in oomycetes

Similar to the work on single fungal hyphae of *N. crassa* (Lew, 2005), the existence of mass flow in the mycelium of the oomycete *A. bisexualis* was examined through the microinjection of silicone oil (Muralidhar et al., 2016). This work was based on the assumption that *A. bisexualis* is unable to turgor regulate (although as noted above this assumption is open to challenge) and that turgor was set simply by the osmotic potential of the media that the hyphae are growing on. Split petri-dishes were used with differing osmolyte concentrations on each side of the dish. A single zoospore was inoculated onto the central partition of the dish, which upon germination and branching formed a mycelium that grew on both sides of the dish. Given the assumed inability to turgor regulate, the coenocytic nature of the oomycete hyphae and the differing osmotic potential media that the hyphae were exposed to on each side of the dish, this was proposed to set up a pressure gradient across the mycelia. To test if this pressure gradient could drive mass flow, silicone oil was microinjected on one side of the dish and was observed to move in the direction as would be predicted by the pressure gradient and thus supporting the existence of mass flow. Furthermore, rates of movement matched tip growth rates and also the rates of oil movement that

would be predicted by the Hagen-Poiseuille equation, however as discussed further below there might be an error in these calculations. In nature the experimental setup could be analogous to a heterogeneous osmotic environment through which the ever-extending edges of the scavenging hyphae experience in the environment (Muralidhar et al., 2016). However, the movement of droplets were slower to that of the organelle movement within mycelia of *A. bisexualis* (Muralidhar et al., 2016). It is not clear what the reason for this might be, but since organelles move via active transport, it might be the result of energy produced during ATP hydrolysis (Muralidhar et al., 2016).

4.6 Mass flow in a single hypha of the oomycete *A. bisexualis*

While the above experiments showed that mass flow could occur within the mycelium of *A. bisexualis*, to the best of my knowledge the existence of mass flow has not been investigated in a single oomycete hypha. Using the same microinjecting method, but a different microinjection apparatus, which included a linear syringe pump, single hypha were tested in the current study. Changes in pressure gradient were achieved by addition of either hyperosmotic or hypoosmotic solutions externally, thus offering a potentially more direct and controlled method of achieving a gradient in a single hypha. Previous studies have suggested that mass flow could be facilitated by minor changes of pressure gradient of the order 0.0005 – 0.1 bar cm^{-1} (Lew, 2005). This correlated to the pressure gradients which were established during this study by the addition of either hyperosmotic (0.064 MPa for 20 µL of 0.5 M sorbitol) solution or hypoosmotic (0.056 MPa for 20 µL of distilled water) solutions externally.

The results from both hyper- and hypoosmotic shock experiments suggest that the process of mass flow might be occurring within a single hypha, as in both cases the oil droplets moved in the predicted direction in the majority of trials. It was also observed that when branches were present close to the region of impalement in the hypha, oil moved into these branches upon establishment of pressure gradients and in the direction predicted. The observations were consistent irrespective of the side of the microinjection site (apical or subapical) at which osmotic challenge was imposed.

However, smaller droplets (below 20 µm diameter) did not show movement after both hypo- and hyperosmotic treatment. The reason for this is not known but it could be suggested to be the

result of a wound response. The wound response has been suggested to have evolved within oomycetes as a mechanism to maintain cell integrity. Callose plugs are accumulated in these coenocytic organisms in case of cellular injury. Upon impalement of the hyphal cells, large number of vesicles were observed to move towards the micropipette and in some cases, lead to its blockage. One theory is that the movement of smaller size droplets was inhibited by the mounting of this wound response and vesicular accumulation around the droplet causing its blockage within the hypha.

In both the earlier study on mycelia (Muralidhar et al., 2016) and now, in this thesis, on individual hypha, in a percentage of trials the oil moved in the opposite direction. For the mycelia it was suggested that if *A. bisexualis* could indeed control turgor to some degree, then they could override the external gradient, which was established using the split petri-dish. In this thesis in 5% of the trials with a hypoosmotic treatment and in 41% of those with a hyperosmotic treatment the oil moved in a direction opposite to that which was predicted. Again, this may be due to the hyphae having gradients present that are greater than the imposed gradients and so the effects of the imposed gradients were not apparent. It is also possible that in the process of adding the hyper- or hypoosmotic solutions the volume of solution added was sufficiently large, that some flowed out of the area where it was applied and in turn this resulted in a possible reversal of the pressure gradient, hence driving the movement of the droplet in the opposite direction.

4.7 PDMS chips to study mass flow

The above highlights the possible need of a more refined means of imposing pressure gradients on individual hyphae. To address this, microfluidic devices were designed and fabricated in an attempt to create a more defined system to study the principle of mass flow within a single hypha. PDMS LOC-chip devices were designed, with inoculation areas and channels of varying widths, allowing for introduction of mycelial plugs onto the devices and the growth of single hyphae along the channels. This enabled the separation of one hypha from the rest of the mycelium. In addition, this design was intended to create a system in which microinjection of a single hypha and solution changes to impose pressure gradients along those hyphae were possible.

While individual hyphae were successfully grown along channels on the LOC devices, unfortunately attempts to inject oil into these hyphae were unsuccessful. This is likely due to the presence of only broth in the channels, which did not offer enough purchase to allow microinjection. Subsequent attempts were made using an invasive method of growth through the addition of media with 1% agar to the channels and inoculation area to offer more stability to the flexible hypha. Earlier studies using a single cell pressure probe have shown that the increased purchase that comes with invasive growth conditions can improve the success rate of impalement (Walker et al., 2006) although this comes with the added difficulty of moving the glass micropipette though the agar media. Unfortunately, in the current experiments the 1% agar was not sufficient to stabilize the hyphae and enable microinjection of oil.

To compensate for this a new chip was designed, which offered more stability to the extended hypha, but due to time constraints this was not able to be tested. It would be of interest to see in the future if this LOC design enables success. Furthermore, it would be of interest to attempt injection of nanoparticles instead of silicone oil droplets to test for mass flow. Nanoparticles have extensively been used in biological models for drug delivery or bioimaging and as biosensors. Due to their size, convenience and availability they might appeal in other biological studies. They have been injected in an attempt to deliver cancer drugs while avoiding the reticuloendothelial system, and also enhancing the specificity of the drug to a particular target site (Brannon-Peppas & Blanchette, 2012). While this might provide an interesting option for the study of mass flow, it should be taken into account that gold nanoparticles have shown toxicity in both *in vivo* and *in vitro* studies. However, to the best of my knowledge this method of studying mass flow has not been tested in fungal or oomycete models and might lead to interesting observations.

4.8 Observed rate of oil movement vs theoretical rates

If we consider the aseptate mycelium of *A. bisexualis* to act as a continuum of pipes, it would be expected that a laminar rather than turbulent flow of material would occur along the hyphae. The Reynold's number would thus ascertain if the flow observed within the hypha is either laminar or turbulent. This was calculated for *N. crassa*, and was approximated at the value of 9.0×10^{-5}, which is low enough to consider the flow to be laminar. To the best of our knowledge this value has not been calculated for *A. bisexualis* or any other oomycete, but considering that fungi and

oomycetes share a lot of similar characteristics, it's likely that the flow occurring within them is laminar as well (Lew, 2005).

Theoretical flow rates for the oil droplets were calculated using the Hagen-Poiseuille equation. The hyphal length and width were measured at the region of impalement during these experiments, while viscosity (η) was taken as 1 X 10^{-3} Pa.s. This viscosity was measured for the cytoplasm of fibroblasts, and was previously used for calculations of mass flow in fungi and oomycetes (Lew, 2005; Muralidhar et al., 2016), although, observations of the oomycete hyphae suggest that their cytoplasm might be more viscous. This value might thus underestimate the viscosity of oomycete cytoplasm. There could also be other factors which might play a role within the hypha to impede the movement of oil droplets such as vacuolation, wound response, and organelles.

Within the mycelia of *A. bisexualis* the measured rates were between 2 X 10^{-8} to 8 X 10^{-8} ms^{-1}, and the theoretical rates were 2.2 X 10^{-8} m s^{-1}, which is within the range of the observed flow value. However, further evaluation of these calculations has suggested that there might be an error and the observed rates are in fact 10 times faster than earlier noted and therefore 10 times faster to that calculated using the equation (0.22 X 10^{-8} m s^{-1}). Results from this study suggest that the observed rates of mass flow within a single hypha are 100 times faster than the theoretical rates during hypoosmotic treatment both apically and subapically. The oil droplet movement rate observed was 3 X 10^{-7} m s^{-1} in the anterograde direction and 4 X 10^{-7} m s^{-1} in the retrograde direction. The theoretical rates were calculated to be 0.23 X 10^{-8} m s^{-1} and 0.29 X 10^{-8} m s^{-1} in the anterograde and retrograde direction respectively. Rate of movement of droplets after hyperosmotic treatment were 1.4 X 10^{-7} m s^{-1} in the retrograde direction while theoretical values were 0.33 X 10^{-8} m s^{-1} were calculated using Hagen-Poiseuille equation, suggesting that the droplets moved 50 times faster than these values. This difference in rates between that observed in the mycelial study and this study, could be the effect of larger pressure gradients established by the direct addition of osmoticum to the desired site of the hyphae. The concentrations of sorbitol used in the mycelial study was 0.3 M while this study used a 0.5 M sorbitol to induce hyperosmotic stress. The increase in observed rates in single hyphae when compared to mycelia could be due to the various cellular elements within the hyphae exerting pressure on the oil droplet to move faster. It could also be the result of a wound response or

vesicle movements towards the tail end of the droplet. Since the oil droplet does not bind to any part of the cytoskeleton, it might be the viscosity of the cytoplasm which could affect the rates within the hyphae. The width of hyphae might also play a role in this increased speed rates, as the hyphae in the mycelial mat are much wider and oil droplets might move at a slower rate when compared to a single hypha at the growing edge, which is narrower. The oil droplets microinjected were larger when compared to those observed in the mycelial study, the forward moving force which is associated with larger mass of the droplet might also affect the increase in movement rates observed.

Even though the observed rates of mass flow are not proportional to the theoretical rates of mass flow, which might be the result of several biological factors working within the hyphae of these organisms, it might still be suggested that mass flow does occur in these organisms. It might be that the hyphae and mycelium act as a continuum of pipes through which cytoplasm flows but other cellular factors in this biological system would influence this flow.

4.9 Summary

To summarize, the objective of this study was to observe if mass flow occurred within a single hypha of the water mold *Achlya bisexualis*. Experimental evidence obtained by the movement of oil droplets in the predicted directions after establishing a pressure gradient by addition of hypo- and hyperosmotic solutions might suggest that mass flow is occurring in a single hypha of these organisms.

The second objective of this thesis was to establish a more streamlined system to study mass flow, which included the production of PDMS microchips with channel widths, which allow the growth of a single hypha, thus isolating it form the rest of the mycelium. This involved designing the above-mentioned devices and processing them for the growth of these oomycetes. Several chip designs and trials lead to growth of isolated hypha on these chips. However, the study of mass flow required the microinjecting of silicone oil droplets and changing of pressure gradients in this microenvironment. Broth alone did not offer enough purchase and invasive methods using 1% agar was also trialed. Growth of the organism was established but even in the invasive condition, the process of microinjecting oil droplets within the hypha was not successful as the presence of 1% agar did not offer enough purchase for this.

Acknowledgements

I cannot thank those who helped me during the course of my thesis enough. Firstly, my supervisors Dr. Ashley Garrill and Dr. Volker Nock, for their academic and technical support. I would also like to thank Allan Woods, Craig Galilee, Mike Shurety and my lab mates. Most importantly I would like to thank both my families for their constant support, especially my pillar of strength Payman for always encouraging me to pursue my dreams.

References

Abadeh, A., & Lew, R. R. (2013). Mass flow and velocity profiles in *Neurospora* hyphae: partial plug flow dominates intra-hyphal transport. *Microbiology (Reading, England), 159*(Pt 11), 2386-2394.

Agudelo, C. G., Sanati Nezhad, A., Ghanbari, M., Naghavi, M., Packirisamy, M., & Geitmann, A. (2013). TipChip: a modular, MEMS-based platform for experimentation and phenotyping of tip-growing cells. *The Plant Journal, 73*(6), 1057-1068.

Amir, R., Levanon, D., Hadar, Y., & Chet, I. (1992). Formation of sclerotia by *Morchella esculenta*: relationship between media composition and turgor potential in the mycelium. *Mycological Research, 96*(11), 943-948.

Amir, R., Levanon, D., Hadar, Y., & Chet, I. (1994). The role of source-sink relationships in translocation during sclerotial formation by *Morchella esculenta*. *Mycological Research, 98*(12), 1409-1414.

Angeles, G., Bond, B., Boyer, J. S., Brodribb, T., Brooks, J. R., Burns, M. J.,Comstock, J. et al (2004). The cohesion-tension theory. *New Phytologist, 163*(3), 451-452.

Arkilic, E. B., Breuer, K. S., & Schmidt, M. A. (2001). Mass flow and tangential momentum accommodation in silicon micromachined channels. *Journal of Fluid Mechanics, 437*, 29-43.

Arkowitz, R. A., & Bassilana, M. (2011). Polarized growth in fungi: symmetry breaking and hyphal formation. *Seminars in Cell Development Biology, 22*(8), 806-815.

Baker, J. M., & van Bavel, C. H. M. (1987). Measurement of mass flow of water in the stems of herbaceous plants. *Plant, Cell and Environment, 10*(9), 777-782.

Baker, J. V., & Bavel, C. V. (1987). Measurement of mass flow of water in the stems of herbaceous plants. *Plant, Cell & Environment, 10*(9), 777-782.

Bartnicki-Garcia, S. (1968). Cell wall chemistry, morphogenesis, and taxonomy of fungi. *Annual Reviews in Microbiology, 22*(1), 87-108.

Bartnicki-García, S. (2002). Hyphal tip growth: outstanding questions. *Mycology Series, 15*, 29-58.

Bartnicki-Garcia, S., & Gierz, G. (1993). Mathematical analysis of the cellular basis of fungal dimorphism. In *Dimorphic Fungi in Biology and Medicine*, 133-144.

Bartnicki-Garcia, S., & Lippman, E. (1969). Fungal morphogenesis: cell wall construction in *Mucor rouxii*. *Science*, *165*(3890), 302-304.

Beakes, G. W., Glockling, S. L., & Sekimoto, S. (2012). The evolutionary phylogeny of the oomycete "fungi". *Protoplasma*, *249*(1), 3-19.

Bebber, D. P., & Gurr, S. J. (2015). Crop-destroying fungal and oomycete pathogens challenge food security. *Fungal Genetics Biology*, *74*, 62-64.

Brannon-Peppas, L., & Blanchette, J. O. (2012). Nanoparticle and targeted systems for cancer therapy. *Advanced drug delivery reviews*, *64*, 206-212.

Chang, F., & Peter, M. (2003). Yeasts make their mark. *Nature cell biology*, *5*(4), 294.

Cosgrove, D., Ortega, J., & Shropshire, W. (1987). Pressure probe study of the water relations of *Phycomyces blakesleeanus* sporangiophores. *Biophysical journal*, *51*(3), 413-423.

Dick, M. (1969). Morphology and taxonomy of the Oomycetes, with special reference to *Saprolegniaceae*, *Leptomitaceae* and *Pythiaceae*. *New Phytologist*, *68*(3), 751-775.

Dixon, H. H., & Joly, J. (1894). On the ascent of sap. *Proceedings of the Royal Society of London*, *57*, 3-5.

Evans, C. S., & Hedger, J. N. (2001). *Degradation of plant cell wall polymers.* Paper presented at the British Mycological Society Symposium Series.

Ewart, T., Perrier, P., Graur, I. A., & Meolans, J. G. (2007). Mass flow rate measurements in a microchannel, from hydrodynamic to near free molecular regimes. *Journal of Fluid Mechanics*, *584*, 337-356.

Fiddy, C., & Trinci, A. (1976). Nuclei, septation, branching and growth of Geotrichum candidum. *Microbiology*, *97*(2), 185-192.

Fischer, M., Cox, J., Davis, D. J., Wagner, A., Taylor, R., Huerta, A. J., & Money, N. P. (2004). New information on the mechanism of forcible ascospore discharge from *Ascobolus immersus*. *Fungal Genetics and Biology*, *41*(7), 698-707.

Fugelstad, J. (2008). *Cellulose Biosynthesis in Oomycetes.*(Licentiate thesis). Retrived from http://www.diva-portal.org/smash/get/diva2:54419/Fulltext01.pdf

Fushimi, K., & Verkman, A. (1991). Low viscosity in the aqueous domain of cell cytoplasm measured by picosecond polarization microfluorimetry. *The Journal of cell biology*, *112*(4), 719-725.

Garrill, A., Lew, R. R., & Heath, I. B. (1992). Stretch-activated Ca^{2+} and Ca^{2+}-activated K^{+} channels in the hyphal tip plasma membrane of the oomycete *Saprolegnia ferax*. *Journal of Cell Science, 101*(3), 721-730.

Gerbore, J., Benhamou, N., Vallance, J., Le Floch, G., Grizard, D., Regnault-Roger, C., & Rey, P. (2014). Biological control of plant pathogens: advantages and limitations seen through the case study of *Pythium oligandrum*. *Environmental Science and Pollution Research, 21*(7), 4847-4860.

Ghanbari, A., Nock, V., Johari, S., Blaikie, R., Chen, X., & Wang, W. (2012). A micropillar-based on-chip system for continuous force measurement of *C. elegans*. *Journal of Micromechanics and Microengineering, 22*(9), 095009.

Goriely, A., & Tabor, M. (2008). Mathematical modeling of hyphal tip growth. *Fungal Biology Reviews, 22*(2), 77-83.

Gould, N., Minchin, P. E., & Thorpe, M. R. (2004). Direct measurements of sieve element hydrostatic pressure reveal strong regulation after pathway blockage. *Functional Plant Biology, 31*(10), 987-993.

Grosse, W., Armstrong, J., & Armstrong, W. (1996). A history of pressurised gas-flow studies in plants. *Aquatic Botany, 54*(2-3), 87-100.

Hakariya, M., Masuyama, N., & Saikawa, M. (2002). Shooting of sporidium by "gun" cells in *Haptoglossa heterospora* and *H. zoospora* and secondary zoospore formation in *H. zoospora*. *Mycoscience, 43*(2), 119-125.

Halldorsson, S., Lucumi, E., Gómez-Sjöberg, R., & Fleming, R. M. (2015). Advantages and challenges of microfluidic cell culture in polydimethylsiloxane devices. *Biosensors and Bioelectronics, 63*, 218-231.

Hardham, A. R., Takemoto, D., & White, R. G. (2008). Rapid and dynamic subcellular reorganization following mechanical stimulation of Arabidopsis epidermal cells mimics responses to fungal and oomycete attack. *BMC plant biology, 8*(1), 63-63.

Harold, R. L., Money, N. P., & Harold, F. M. (1996). Growth and morphogenesis in *Saprolegnia ferax*: Is turgor required? *Protoplasma, 191*(1-2), 105-114.

Harris, G. F. (2006). Te paraiti: The 1905-1906 potato blight epidemic in New Zealand and its effects on Maori communities.
Retrived from https://repository.openpolytechnic.ac.nz/handle/11072/1212

Harris, S. D. (2008). Branching of fungal hyphae: regulation, mechanisms and comparison with other branching systems. *Mycologia, 100*(6), 823-832.

Harris, S. D. (2011). Hyphal morphogenesis: an evolutionary perspective. *Fungal biology, 115*(6), 475-484.

Harris, S. D., Hofmann, A. F., Tedford, H. W., & Lee, M. P. (1999). Identification and characterization of genes required for hyphal morphogenesis in the filamentous fungus *Aspergillus nidulans*. *Genetics, 151*(3), 1015-1025.

Heath, I. B. (1982). The effect of nocodazole on the growth and ultrastructure of the fungus *Saprolegnia ferax*. Evidence against a simple mode of action. *Microtubules in Microorganisms*, 275-311.

Herr, F. B., & Heath, M. C. (1982). The effects of antimicrotubule agents on organelle positioning in the cowpea rust fungus, *Uromyces phaseoli* var. vignae. *Experimental mycology, 6*(1), 15-24.

Hoch, H., & Staples, R. (1983). Ultrastructural organization of the non-differentiated uredospore germling of *Uromyces phaseoli* variety typica. *Mycologia*, 795-824.

Howard, R. J. (1981). Ultrastructural analysis of hyphal tip cell growth in fungi: Spitzenkorper, cytoskeleton and endomembranes after freeze-substitution. *Journal of Cell Science, 48*(1), 89-103.

Howard, R. J., Ferrari, M. A., Roach, D. H., & Money, N. P. (1991). Penetration of hard substrates by a fungus employing enormous turgor pressures. *Proceedings of the National Academy of Sciences, 88*(24), 11281-11284.

Jennings, D. (1987). Translocation of solutes in fungi. *Biological Reviews, 62*(3), 215-243.

Johari, S., Nock, V., Alkaisi, M. M., & Wang, W. (2013). On-chip analysis of C. elegans muscular forces and locomotion patterns in microstructured environments. *Lab on a Chip, 13*(9), 1699-1707.

Kaminskyj, S. G., Garrill, A., & Heath, I. B. (1992). The relation between turgor and tip growth in *Saprolegnia ferax*: turgor is necessary, but not sufficient to explain apical extension rates. *Experimental mycology, 16*(1), 64-75.

Kamoun, S. (2003). Molecular genetics of pathogenic oomycetes. *Eukaryotic cell, 2*(2), 191-199.

Kamoun, S., Furzer, O., Jones, J. D., Judelson, H. S., Ali, G. S., Dalio, R. J.,Panabières, F et al. (2015). The Top 10 oomycete pathogens in molecular plant pathology. *Molecular plant pathology, 16*(4), 413-434.

Knoblauch, M., Peters, W. S., Ehlers, K., & van Bel, A. J. (2001). Reversible calcium-regulated stopcocks in legume sieve tubes. *The Plant Cell, 13*(5), 1221-1230.

Köckenberger, W., Pope, J., Xia, Y., Jeffrey, K., Komor, E., & Callaghan, P. (1997). A non-invasive measurement of phloem and xylem water flow in castor bean seedlings by nuclear magnetic resonance microimaging. *Planta, 201*(1), 53-63.

Lang, A. (1983). Turgor-regulated translocation. *Plant, Cell & Environment*, 6(9), 683-689.

Latijnhouwers, M., de Wit, P. J., & Govers, F. (2003). Oomycetes and fungi: similar weaponry to attack plants. *Trends in Microbiology, 11*(10), 462-469.

Lehmler, C., Steinberg, G., Snetselaar, K. M., Schliwa, M., Kahmann, R., & Bölker, M. (1997). Identification of a motor protein required for filamentous growth in *Ustilago maydis*. *The European Molecular Biology Organisation journal, 16*(12), 3464-3473.

Lemmon, M. A. (2003). Phosphoinositide recognition domains. *Traffic, 4*(4), 201-213.

Lévesque, C. A. (2011). Fifty years of oomycetes—from consolidation to evolutionary and genomic exploration. *Fungal Diversity, 50*(1), 35-46.

Levina, N., Heath, I., & Lew, R. (2000). Rapid wound responses of *Saprolegnia ferax* hyphae depend upon actin and Ca^{2+}-involving deposition of callose plugs. *Protoplasma, 214*(3), 199-209.

Lew, R. R. (1994). Regulation of electrical coupling between Arabidopsis root hairs. *Planta, 193*(1), 67-73.

Lew, R. R. (2005). Mass flow and pressure-driven hyphal extension in *Neurospora crassa*. *Microbiology, 151*(8), 2685-2692.

Lew, R. R. (2011). How does a hypha grow? The biophysics of pressurized growth in fungi. *Nature Reviews Microbiology, 9*(7), 509-518.

Lew, R. R., Levina, N. N., Walker, S. K., & Garrill, A. (2004). Turgor regulation in hyphal organisms. *Fungal Genetics and Biology, 41*(11), 1007-1015.

Li, W., Zhang, T., Tang, X., & Wang, B. (2010). Oomycetes and fungi: important parasites on marine algae. *Acta Oceanologica Sinica, 29*(5), 74-81.

López-Franco, R., & Bracker, C. E. (1996). Diversity and dynamics of the Spitzenkörper in growing hyphal tips of higher fungi. *Protoplasma, 195*(1-4), 90-111.

Losev, E., Reinke, C. A., Jellen, J., Strongin, D. E., Bevis, B. J., & Glick, B. S. (2006). Golgi maturation visualized in living yeast. *Nature, 441*(7096), 1002.

MacRobbie, E. A. (1971). Fluxes and compartmentation in plant cells. *Annual Review of Plant Physiology, 22*(1), 75-96.

Mendoza, L., & Vilela, R. (2013). The Mammalian Pathogenic Oomycetes. *Current Fungal Infection Reports, 7*(3), 198-208.

Minchin, P. E., & Thorpe, M. R. (2003). Using the short-lived isotope 11C in mechanistic studies of photosynthate transport. *Functional Plant Biology, 30*(8), 831-841.

Money, N. P. (1990). Measurement of hyphal turgor. *Experimental mycology, 14*(4), 416-425.

Money, N. P. (2008). Insights on the mechanics of hyphal growth. *Fungal Biology Reviews, 22*(2), 71-76.

Money, N. P. (2011). Introduction: The 200th anniversary of the hypha. *Fungal biology, 115*(6), 443-445.

Money, N. P., & Harold, F. M. (1992). Extension growth of the water mold *Achlya*: interplay of turgor and wall strength. *Proceedings of the National Academy of Sciences, 89*(10), 4245-4249.

Money, N. P., & Harold, F. M. (1993). Two water molds can grow without measurable turgor pressure. *Planta, 190*(3), 426-430.

Money, N. P., & Howard, R. J. (1996). Confirmation of a link between fungal pigmentation, turgor pressure, and pathogenicity using a new method of turgor measurement. *Fungal Genetics and Biology, 20*(3), 217-227.

Munch, E. (1930). Stoffbewegungen in der Pflanze.

Munnik, T., & Vermeer, J. E. (2010). Osmotic stress-induced phosphoinositide and inositol phosphate signalling in plants. *Plant, Cell & Environment, 33*(4), 655-669.

Muralidhar, A., Novis, P. M., Broady, P. A., Collings, D. A., & Garrill, A. (2013). An estuarine species of the alga *Vaucheria* (Xanthophyceae) displays an increased capacity for turgor regulation when compared to a freshwater species. *Journal of phycology, 49*(5), 967-978.

Muralidhar, A., Shabala, L., Broady, P., Shabala, S., & Garrill, A. (2015). Mechanisms underlying turgor regulation in the estuarine alga *Vaucheria erythrospora*

(Xanthophyceae) exposed to hyperosmotic shock. *Plant, Cell & Environment*, *38*(8), 1514-1527.

Muralidhar, A., Swadel, E., Spiekerman, M., Suei, S., Fraser, M., Ingerfeld, M., A. Tayagui, Garrill, A. (2016). A pressure gradient facilitates mass flow in the oomycete *Achlya bisexualis*. *Microbiology*, *162*(2), 206-213.

Nakagiri, A. (2000). Ecology and biodiversity of Halophytophthora species. *Fungal Diversity*, *5*, 153-164.

Osiewacz, H. D. (2002). *Molecular biology of fungal development* (Vol. 15): CRC Press.

Peñalva, M. A., Galindo, A., Abenza, J. F., Pinar, M., Calcagno-Pizarelli, A. M., Arst, H. N., & Pantazopoulou, A. (2012). Searching for gold beyond mitosis: mining intracellular membrane traffic in *Aspergillus nidulans*. *Cellular logistics*, *2*(1), 2-14.

Ramos-García, S. L., Roberson, R. W., Freitag, M., Bartnicki-García, S., & Mouriño-Pérez, R. R. (2009). Cytoplasmic Bulk Flow Propels Nuclei in Mature Hyphae of *Neurospora crassa*. *Eukaryotic cell*, *8*(12), 1880.

Randall, T. A., Dwyer, R. A., Huitema, E., Beyer, K., Cvitanich, C., Kelkar, H.,Yatzkan, E *et.al*. (2005). Large-scale gene discovery in the oomycete *Phytophthora infestans* reveals likely components of phytopathogenicity shared with true fungi. *Molecular Plant-Microbe Interactions*, *18*(3), 229-243.

Read, N. D., & Kalkman, E. R. (2003). Does endocytosis occur in fungal hyphae? *Fungal Genetics and Biology*, *39*(3), 199-203.

Reynaga-Peña, C. G., Gierz, G., & Bartnicki-Garcia, S. (1997). Analysis of the role of the Spitzenkörper in fungal morphogenesis by computer simulation of apical branching in *Aspergillus niger*. *Proceedings of the National Academy of Sciences*, *94*(17), 9096-9101.

Riquelme, M. (2013). Tip growth in filamentous fungi: a road trip to the apex. *Annual review of microbiology*, *67*, 587-609.

Riquelme, M., Bartnicki-García, S., González-Prieto, J. M., Sánchez-León, E., Verdín-Ramos, J. A., Beltrán-Aguilar, A., & Freitag, M. (2007). Spitzenkörper localization and intracellular traffic of green fluorescent protein-labeled CHS-3 and CHS-6 chitin synthases in living hyphae of *Neurospora crassa*. *Eukaryotic cell*, *6*(10), 1853-1864.

Robertson, N. F., & Rizvi, S. R. H. (1968). Some Observations on the Water-Relations of the Hyphae of *Neurospora crassa*. *Annals of Botany*, *32*(2), 279-291.

Rokitta, M., Peuke, A., Zimmermann, U., & Haase, A. (1999). Dynamic studies of phloem and xylem flow in fully differentiated plants by fast nuclear-magnetic-resonance microimaging. *Protoplasma, 209*(1-2), 126-131.

Salogiannis, J., & Reck-Peterson, S. L. (2017). Hitchhiking: a non-canonical mode of microtubule-based transport. *Trends in cell biology, 27*(2), 141-150.

Shabala, S. N., & Lew, R. R. (2002). Turgor regulation in osmotically stressed Arabidopsis epidermal root cells. Direct support for the role of inorganic ion uptake as revealed by concurrent flux and cell turgor measurements. *Plant physiology, 129*(1), 290-299.

Smith, A. M., & Callow, J. A. (2006). *Biological adhesives* (Vol. 23): Springer.

Smith, D., & Allen, S. (1996). Measurement of sap flow in plant stems. *Journal of Experimental Botany, 47*(12), 1833-1844.

Srivastava, G. (1967). Ecological studies on some aquatic fungi of Gorakhpur, India. *Hydrobiologia, 30*(3-4), 385-404.

Stajich, J. E., Berbee, M. L., Blackwell, M., Hibbett, D. S., James, T. Y., Spatafora, J. W., & Taylor, J. W. (2009). Primer--The Fungi. *Current biology: CB, 19*(18), R840.

Steinberg, G. (2014). Endocytosis and early endosome motility in filamentous fungi. *Current opinion in microbiology, 20*, 10-18.

Steinberg, G., Peñalva, M. A., Riquelme, M., Wosten, H., & Harris, S. D. (2017). Cell biology of hyphal growth. *Microbiology spectrum, 5*(2), 1-34.

Steinberg, G., & Schliwa, M. (1993). Organelle movements in the wild type and wall-less fz; sg; os-1 mutants of *Neurospora crassa* are mediated by cytoplasmic microtubules. *Journal of Cell Science, 106*(2), 555-564.

Suei, S., & Garrill, A. (2008). An F-actin-depleted zone is present at the hyphal tip of invasive hyphae of *Neurospora crassa*. *Protoplasma, 232*(3-4), 165.

Takeshita, N., Higashitsuji, Y., Konzack, S., & Fischer, R. (2008). Apical sterol-rich membranes are essential for localizing cell end markers that determine growth directionality in the filamentous fungus *Aspergillus nidulans*. *Molecular biology of the cell, 19*(1), 339-351.

Tayagui, A., Sun, Y., Collings, D. A., Garrill, A., & Nock, V. (2017). An elastomeric micropillar platform for the study of protrusive forces in hyphal invasion. *Lab on a Chip, 17*(21), 3643-3653.

Thines, M., & Kamoun, S. (2010). Oomycete-plant coevolution: recent advances and future prospects. *Current Opinion Plant Biology*, *13*(4), 427-433.

Tomos, A. D., & Leigh, R. A. (1999). The pressure probe: a versatile tool in plant cell physiology. *Annual review of plant biology*, *50*(1), 447-472.

Van As, H., & Schaafsma, T. (1984). Noninvasive measurement of plant water flow by nuclear magnetic resonance. *Biophysical journal*, *45*(2), 469-472.

van Bel, A. J. (2003). The phloem, a miracle of ingenuity. *Plant, Cell & Environment*, *26*(1), 125-149.

Verdín, J., Bartnicki-Garcia, S., & Riquelme, M. (2009). Functional stratification of the Spitzenkörper of *Neurospora crassa*. *Molecular microbiology*, *74*(5), 1044-1053.

Vida, T. A., & Emr, S. D. (1995). A new vital stain for visualizing vacuolar membrane dynamics and endocytosis in yeast. *The Journal of cell biology*, *128*(5), 779-792.

Walker, S. K., Chitcholtan, K., Yu, Y., Christenhusz, G. M., & Garrill, A. (2006). Invasive hyphal growth: an F-actin depleted zone is associated with invasive hyphae of the oomycetes *Achlya bisexualis* and *Phytophthora cinnamomi*. *Fungal Genetics and Biology*, *43*(5), 357-365.

Wang, L., Hukin, D., Pritchard, J., & Thomas, C. (2006). Comparison of plant cell turgor pressure measurement by pressure probe and micromanipulation. *Biotechnology Letters*, *28*(15), 1147-1150.

Wei, C., Tyree, M. T., & Steudle, E. (1999). Direct measurement of xylem pressure in leaves of intact maize plants. A test of the cohesion-tension theory taking hydraulic architecture into consideration. *Plant physiology*, *121*(4), 1191-1205.

Wessels, J. (1988). A steady-state model for apical wall growth in fungi. *Plant Biology*, *37*(1), 3-16.

Windt, C. W., Vergeldt, F. J., De Jager, P. A., & Van As, H. (2006). MRI of long-distance water transport: a comparison of the phloem and xylem flow characteristics and dynamics in poplar, castor bean, tomato and tobacco. *Plant, Cell & Environment*, *29*(9), 1715-1729.

Wooding, S., & Pelham, H. R. (1998). The dynamics of Golgi protein traffic visualized in living yeast cells. *Molecular biology of the cell*, *9*(9), 2667-2680.

Xu, J.-R., & Hamer, J. E. (1996). MAP kinase and cAMP signaling regulate infection structure formation and pathogenic growth in the rice blast fungus *Magnaporthe grisea*. *Genes & development, 10*(21), 2696-2706.

Xu, J.-R., Staiger, C. J., & Hamer, J. E. (1998). Inactivation of the Mitogen-Activated Protein Kinase Mps1 from the Rice Blast Fungus Prevents Penetration of Host Cells but Allows Activation of Plant Defense Responses. *Proceedings of the National Academy of Sciences of the United States of America, 95*(21), 12713-12718.

Yoon, E., & Wise, K. D. (1992). An integrated mass flow sensor with on-chip CMOS interface circuitry. *IEEE Transactions on Electron Devices, 39*(6), 1376-1386.

Yoshida, K., Schuenemann, V. J., Cano, L. M., Pais, M., Mishra, B., Sharma, R.,Krause, J *et. al*. (2013). The rise and fall of the *Phytophthora infestans* lineage that triggered the Irish potato famine. *Elife, 2*.

Yu, Y. P., Jackson, S. L., & Garrill, A. (2004). Two distinct distributions of F-actin are present in the hyphal apex of the oomycete *Achlya bisexualis*. *Plant and cell physiology, 45*(3), 275-280.

Ziegler, H. (1975). Nature of transported substances. In *Transport in Plants I* (pp. 59-100): Springer.